

STEADY-
STATE DETERMINATION OF CONTINUOUS POWDER MIXING BY NEAR INFRARED SPECT
ROSCOPY AS PROCESS ANALYTICAL TECHNOLOGY



A Thesis Submitted in Partial Fulfillment of the Requirements
for the Degree of Master of Science in Pharmacy in Industrial Pharmacy
Department of Pharmaceutics and Industrial Pharmacy
Faculty of Pharmaceutical Sciences
Chulalongkorn University
Academic Year 2018
Copyright of Chulalongkorn University

การตรวจสอบภาวะคงที่ของการผสมแบบต่อเนื่องด้วยเนียร์อินฟราเรดสเปกโทรสโกปีสำหรับเป็น
เทคโนโลยีการวิเคราะห์กระบวนการ



วิทยานิพนธ์นี้เป็นส่วนหนึ่งของการศึกษาตามหลักสูตรปริญญาเภสัชศาสตรมหาบัณฑิต
สาขาวิชาเภสัชอุตสาหกรรม ภาควิชาวิทยาการเภสัชกรรมและเภสัชอุตสาหกรรม
คณะเภสัชศาสตร์ จุฬาลงกรณ์มหาวิทยาลัย
ปีการศึกษา 2561
ลิขสิทธิ์ของจุฬาลงกรณ์มหาวิทยาลัย

เกชราภรณ์ ว่องเวศน์ : การตรวจหาสถานะคงที่ของการผสมผงแบบต่อเนื่องด้วยเนียร์อินฟราเรดสเปกโทรสโกปีสำหรับเป็นเทคโนโลยีการวิเคราะห์กระบวนการ. (STEADY-STATE DETERMINATION OF CONTINUOUS POWDER MIXING BY NEAR INFRARED SPECTROSCOPY AS PROCESS ANALYTICAL TECHNOLOGY) อ.ที่ปรึกษาหลัก : อ. ภาณุ. ดร.นฤพร สุทัศน์วิบูลย์, อ.ที่ปรึกษาร่วม : ผศ. ภาณุ. ดร.จิตติมา ชัชวาลย์สายสินธ์

การผสมแบบผงแห้งเป็นหนึ่งในหน่วยการผลิตที่สำคัญในการผลิตเภสัชภัณฑ์ในรูปแบบของแข็ง การผสมแบบต่อเนื่องเป็นวิธีที่ได้ถูกพัฒนาขึ้นเพื่อลดข้อเสียที่เกิดจากกระบวนการผสมในปัจจุบัน กระบวนการผสมแบบต่อเนื่องมักจะพัฒนาโดยใช้เครื่องผสมในแนวนอนและมีการติดตามกระบวนการแบบเวลาจริงโดยใช้เครื่องมือเทคโนโลยีการวิเคราะห์กระบวนการ (พีเอที) งานวิจัยนี้ได้มีการพัฒนาและประเมินเครื่องผสมในแนวตั้ง โดยข้อมูลเนียร์อินฟราเรดสเปกตรัมที่ได้จากการติดตามกระบวนการผสมในช่วงคลื่น $6800 - 8700 \text{ cm}^{-1}$ จะถูกนำมาปรับแต่งด้วยวิธีการปรับแก้การกระเจิงแบบผลคูณ (เอ็มเอสซี) อนุพันธ์ลำดับที่สอง และปรับเรียบข้อมูลด้วยวิธีอินอร์ริส-วิลเลียม ก่อนจะนำไปสร้างเป็นสมการด้วยวิธีกำลังสองน้อยที่สุดบางส่วน (พีแอลเอส) โดยใช้การวิเคราะห์ด้วยการเบี่ยงเบนรังสีเอกซ์ (เอกซ์อาร์ดี) เป็นวิธีปฐมภูมิ ได้มีการติดตามความเข้มข้นของสารผสมในช่วงสถานะคงที่และรูปแบบของการผสมหลังจากมีการปรับเปลี่ยนวิธีการจัดเรียงใบพัด (ทิศทางเดียวกันและสลับ) และระยะห่างระหว่างใบพัด (0.5 และ 1.0 นิ้ว) จากการศึกษาพบว่าวิธีการจัดเรียงใบพัดและระยะห่างระหว่างใบพัดส่งผลกระทบต่อคุณภาพของการผสม มีการประเมินสถานะคงที่ของการผสม ระยะเวลาเริ่มต้นที่เข้าสู่สถานะคงที่ ประสิทธิภาพในการผสม วิธีการวัดที่ไม่ไวต่อการเปลี่ยนแปลง และ ความแม่นยำของความเข้มข้นของสารผสมสุดท้าย พบว่าการจัดเรียงใบพัดทิศทางเดียวกันที่ระยะห่างระหว่างใบพัด 0.5 นิ้วส่งผลให้เกิดความสม่ำเสมอของการผสมที่สูงขึ้น แต่อย่างไรก็ตามจะส่งผลในเชิงลบต่อระยะเวลาในการเข้าสู่สถานะคงที่

CHULALONGKORN UNIVERSITY

สาขาวิชา เภสัชอุตสาหกรรม

ปีการศึกษา 2561

ลายมือชื่อนิสิต

ลายมือชื่อ อ.ที่ปรึกษาหลัก

ลายมือชื่อ อ.ที่ปรึกษาร่วม

5876102033 : MAJOR INDUSTRIAL PHARMACY

KEYWORD: Near infrared spectroscopy, Continuous powder mixing, Process analytical technology, PLS, Vertical continuous powder mixer

Katesaraporn Wongves : STEADY-STATE DETERMINATION OF CONTINUOUS POWDER MIXING BY NEAR INFRARED SPECTROSCOPY AS PROCESS ANALYTICAL TECHNOLOGY . Advisor: Narueporn Sutanthavibul, Ph.D. Co-advisor: Asst. Prof. Jittima Chatchawalsaisin, Ph.D.

Powder mixing is one of an important unit operation in pharmaceutical manufacturing of solid dosage forms. Continuous mixing was developed as an alternative method to reduce disadvantages of traditional batch mixing processes. This process was originally developed using horizontal cylindrical mixer equipped with Process Analytical Technology (PAT) tools for real-time monitoring. In the present study, a vertical cylindrical mixer was developed and evaluated. Near Infrared (NIR) spectra obtained by monitoring the mixing process were pretreated with Multiplicative Scatter Correction (MSC), second derivative treatment and Norris-William smoothing in the 6800 - 8700 cm^{-1} range before a calibration model using PLS was developed using X-ray powder diffractometry (XRPD) as a primary method. Concentrations of mixtures in steady-state and mixing phases were identified after changing impeller alignments (aligned and opposite) and distances between impellers (0.5 and 1.0 inch). Blend quality was found to be affected by both the impeller alignment and impeller distance. Steady-state phases, onset time, mixing performance, measurement robustness and accuracy of final mixture concentrations were evaluated. It was found that aligned impeller with 0.5-inch distance shows the best mixing set-up leading to higher mixture homogeneity. However, onset time to reach steady-state was compromised.

Field of Study: Industrial Pharmacy

Academic Year: 2018

Student's Signature

Advisor's Signature

Co-advisor's Signature

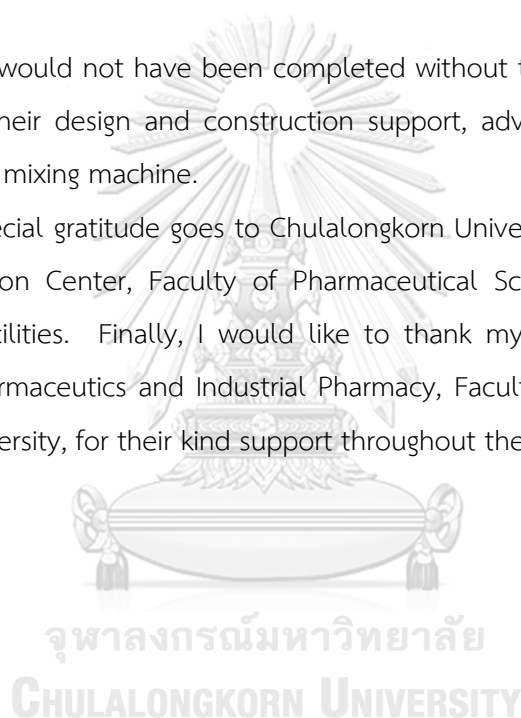
ACKNOWLEDGEMENTS

I would like to express my sincere gratitude to my thesis advisor, Dr. Narueporn Sutanthavibul for her invaluable help, patience, and immense knowledge throughout this research. Besides my advisor, I would like to thank my thesis co-advisor, Assistant Professor Jittima Chatchawalsaisin for her grateful advice, teaching and encouragement.

My sincere thanks also extended to Dr. Sumaporn Kasamsumran for her suggestions with NIRs technique. Without her suggestions, my thesis could not have been successfully completed.

My thesis would not have been completed without the support of my family. I am most grateful for their design and construction support, advise and all their help on the continuous powder mixing machine.

A very special gratitude goes to Chulalongkorn University Drug and Health Products Innovation Promotion Center, Faculty of Pharmaceutical Sciences, for providing research equipment and facilities. Finally, I would like to thank my classmates and staffs in the Department of Pharmaceutics and Industrial Pharmacy, Faculty of Pharmaceutical Sciences, Chulalongkorn University, for their kind support throughout the period of my research career.



Katesaraporn Wongves

TABLE OF CONTENTS

	Page
.....	iii
ABSTRACT (THAI).....	iii
.....	iv
ABSTRACT (ENGLISH).....	iv
ACKNOWLEDGEMENTS.....	v
TABLE OF CONTENTS.....	vi
CHAPTER I.....	1
INTRODUCTION.....	1
CHAPTER II.....	4
LITERATURE REVIEW.....	4
1. Pharmaceutical manufacturing.....	4
2. Solid mixing.....	7
3. Process analytical technology (PAT).....	14
4. Implementing NIRs in continuous mixing process.....	19
5. Direct compressible excipients.....	21
CHAPTER III.....	23
MATERIALS AND METHOD.....	23
1. Material selection.....	23
2. Vertical continuous powder mixer.....	24
2.1. Structure.....	24
2.2. Vertical continuous powder mixer operating principles.....	25

3.	NIR calibration model development	25
3.1.	Preparation of calibration samples.....	26
3.2.	XRPD analysis	26
3.3.	NIR data processing.....	26
4.	Real-time continuous mixing process monitoring, data processing and analysis	
	28	
4.1.	Set-up for real-time continuous mixing process monitoring.....	28
4.2.	NIR spectral measurements	31
4.3.	Data processing and analysis	31
CHAPTER VI	32
RESULTS AND DISCUSSIONS	32
1.	Materials selection.....	32
2.	NIR calibration model development	34
2.1.	XRPD analysis	34
2.2.	NIR calibration model development.....	37
3.	Real-time continuous mixing process monitoring.....	46
3.1.	Onset time of steady-state.....	58
3.2.	Mixing performance.....	59
3.3.	Target concentration reached in real-time measurement.....	60
3.4.	Accuracy of final target concentration mixtures.....	61
CHAPTER V	63
CONCLUSION	63
APPENDIX	67
REFERENCES	2

VITA..... 7



จุฬาลงกรณ์มหาวิทยาลัย
CHULALONGKORN UNIVERSITY

TABLE OF CONTENTS

	Page
ABSTRACT (THAI)	iii
ABSTRACT (ENGLISH)	iv
ACKNOWLEDGEMENTS	v
TABLE OF CONTENTS	vi
LIST OF TABLES	ix
LIST OF FIGURES	x
ABSTRACT (THAI)	iii
ABSTRACT (ENGLISH)	iv
ACKNOWLEDGEMENTS	v
TABLE OF CONTENTS	vi
CHAPTER I	1
INTRODUCTION	1
CHAPTER II	4
LITERATURE REVIEW	4
1. Pharmaceutical manufacturing	4
2. Solid mixing	7
3. Process analytical technology (PAT)	14
4. Implementing NIRs in continuous mixing process	19
5. Direct compressible excipients	21
CHAPTER III	23
MATERIALS AND METHOD	23
1. Material selection	23

2. Vertical continuous powder mixer	24
2.1. Structure	24
2.2. Vertical continuous powder mixer operating principles	25
3. NIR calibration model development	25
3.1. Preparation of calibration samples	26
3.2. XRPD analysis	26
3.3. NIR data processing	26
4. Real-time continuous mixing process monitoring, data processing and analysis	28
4.1. Set-up for real-time continuous mixing process monitoring	28
4.2. NIR spectral measurements	31
4.3. Data processing and analysis	31
CHAPTER VI	32
RESULTS AND DISCUSSIONS	32
1. Materials selection	32
2. NIR calibration model development	34
2.1. XRPD analysis	34
2.2. NIR calibration model development	37
3. Real-time continuous mixing process monitoring	46
3.1. Onset time of steady-state	58
3.2. Mixing performance	59
3.3. Target concentration reached in real-time measurement	60
3.4. Accuracy of final target concentration mixtures	61
CHAPTER V	63

CONCLUSION63

APPENDIX67

REFERENCES72

VITA76



LIST OF TABLES

	Page
Table 3-1 Pretreatment methods for NIR spectra.	27
Table 3-2 Mixing impeller set-up for each trial.....	30
Table 4-1 Spectral range used for developing NIR calibration model	41
Table 4-2 Pretreatment of NIR calibration model in the region of 6800 - 8700 cm^{-1}	45



LIST OF FIGURES

	Page
Figure 2-1 Flow diagram of typical oral solid dosage manufacturing(12)	4
Figure 2-2 States of mixtures.....	8
Figure 2-3 Segregation patterns between large (light) and small (dark) grains	8
Figure 2-4 Batch processing.....	9
Figure 2-5 Three types of tumbler mixer: (A) double cone (B) V-blender (C) bin blender (19).	10
Figure 2-6 Example of convective mixer: ribbon blender(19).....	10
Figure 2-7 Continuous processing	11
Figure 2-8 GCM continuous mixer from Gericke(22).....	12
Figure 2-9 Continuous modular mixer (Modulomix) from Hosokawa Micron B.V.(23)..	12
Figure 2-10 Process parameters in continuous powder mixer(11).	13
Figure 2-11 SEM photomicrograph of spray dried lactose (Flowlac [®] 100)(36).....	21
Figure 2-12 SEM photomicrograph of Pregelatinized starch (Starch 1500 [®])(37).	21
Figure 2-13 SEM photomicrograph of microcrystalline cellulose PH 102 (CEOLUS [®] PH 102)(38).....	22
Figure 3-1 Machine structure.....	25
Figure 3-2 Experimental setup for obtaining NIR calibration model.....	26
Figure 3-3 Experimental setup for monitoring continuous powder mixing process.	28
Figure 3-4 Mixing impeller configurations and NIR fiber-optic probe positions.	29
Figure 4-1 Iron powder used in the experiment	32
Figure 4-2 Particle size distribution of iron powder.....	33
Figure 4-3 Hausner ratios and flow characters of directly compressible excipients. ...	34

Figure 4-4 XRPD diffraction pattern of iron powder	35
Figure 4-5 XRPD diffraction pattern of spray dried lactose (FlowLac® 100).....	36
Figure 4-6 XRPD diffraction patterns of spray dried lactose in iron powder physical mixtures of known concentrations.	36
Figure 4-7 Calibration curve of XRPD intensity at 20 °2θ and concentrations of spray dried lactose in spray dried lactose/iron powder physical mixtures.....	37
Figure 4-8 NIR spectra of pure iron powder (A) and spray dried lactose (B).....	38
Figure 4-9 NIR spectra of iron powder, spray dried lactose and 20% to 90% (w/w) spray dried lactose/iron powder physical mixtures.	38
Figure 4-10 NIR calibration model between wavenumber at 4000 – 10000 cm ⁻¹	39
Figure 4-11 NIR calibration model between wavenumber at 4000 – 6000 cm ⁻¹	40
Figure 4-12 NIR calibration model between wavenumber at 4000 – 7600 cm ⁻¹	40
Figure 4-13 NIR calibration model between wavenumber at 6800 – 8700 cm ⁻¹	41
Figure 4-14 Calibration model (in-set) and non-treated of NIR spectra.....	42
Figure 4-15 Calibration model (in-set) of NIR spectra after MSC pretreatment.....	43
Figure 4-16 Calibration model (in-set) of NIR spectra after 2 nd derivative + Norris-Williams pretreatment	43
Figure 4-17 Calibration model (in-set) of NIR spectra after MSC + 2 nd derivative + Norris-Williams pretreatment	44
Figure 4-18 In-house vertical mixer for continuous mixing process.....	46
Figure 4-19 Predicted NIR concentrations in trial A.....	49
Figure 4-20 %RSD of moving block concentrations average from trial A.	49
Figure 4-21 Predicted NIR concentrations in trial B.....	50
Figure 4-22 %RSD of moving block concentrations average from trial B.	50
Figure 4-23 Predicted NIR concentrations in trial C.....	51

Figure 4-24 %RSD of moving block concentrations average from trial C.	51
Figure 4-25 Predicted NIR concentrations in trial D.....	52
Figure 4-26 %RSD of moving block concentrations average from trial D.	52
Figure 4-27 Predicted NIR concentrations in trial E.	53
Figure 4-28 %RSD of moving block concentrations average from trial E.....	53
Figure 4-29 Predicted NIR concentrations in trial F.	54
Figure 4-30 %RSD of moving block concentrations average from trial F.....	54
Figure 4-31 Predicted NIR concentrations in trial G.....	55
Figure 4-32 %RSD of moving block concentrations average from trial G.	55
Figure 4-33 Predicted NIR concentrations in trial H.....	56
Figure 4-34 %RSD of moving block concentrations average from trial H.	56
Figure 4-35 Concentrations of three phases of trial H during continuous mixing process obtained by NIR: Initial, steady state and depletion.	57
Figure 4-36 Steady-state reached in each trial.....	58
Figure 4-37 Statistical comparisons of average mixture concentrations from trial A to H and concentration final mixtures collected at the outlet during steady-state.....	59
Figure 4-38 Mixture concentrations during steady-state.	60
Figure 4-39 Final mixture concentrations collected from outlet during steady-state.	62
Figure A-1 Calibration model of no. 1 with no pretreatment.....	67
Figure A-2 Calibration model of no.2 with 1 st derivative + Norris-Williams pretreatment	67
Figure A-3 Calibration model of no.3 with 1 st derivative + Savitzky-Golay pretreatment	67
Figure A-4 Calibration model of no.4 with 2 nd derivative + Norris-Williams pretreatment	68

Figure A-5 Calibration model of no.5 with 2 nd derivative + Savitzky-Golay pretreatment	68
Figure A-6 Calibration model of no.6 with MSC pretreatment	68
Figure A-7 Calibration model of no.7 with SNV pretreatment	69
Figure A-8 Calibration model of no.8 with MSC + 1 st derivative + Norris-Williams pretreatment	69
Figure A-9 Calibration model of no.9 with MSC + 1 st derivative + Savitzky-Golay pretreatment	69
Figure A-10 Calibration model of no.10 with MSC + 2 nd derivative + Norris-Williams pretreatment	70
Figure A-11 Calibration model of no.11 with MSC + 2 nd derivative + Savitzky-Golay pretreatment	70
Figure A-12 Calibration model of no.12 with SNV + 1 st derivative + Norris-Williams pretreatment	70
Figure A-13 Calibration model of no.13 with SNV + 1 st derivative + Savitzky-Golay pretreatment	71
Figure A-14 Calibration model of no.14 with SNV + 2 nd derivative + Norris-Williams pretreatment	71
Figure A-15 Calibration model of no.15 with SNV + 2 nd derivative + Savitzky-Golay pretreatment	71

CHAPTER I

INTRODUCTION

Recently, there has been growing interest in continuous processing in pharmaceutical manufacturing. Continuous processing is a common process for many industries such as bulk chemical, petrochemicals and starch manufacture. From the final report on Pharmaceutical Quality for the Twenty-first Century, the vision for The United States Food and Drug Administration (U.S. FDA)'s pharmaceutical quality initiative is to produce high-quality drugs with an agile, flexible and reliable pharmaceutical manufacturing without extensive regulatory oversight(1). This vision promotes the adoption of continuous processing in the pharmaceutical industry.

Continuous processing is a modern manufacturing approach that offers a great potential to build the quality into process design, in research and development and improve quality of drug manufacturing. Compare to batch processing, this processing offers several advantages and opportunities to enhance the quality of both process and product(2).

Mixing operation is one of an important unit operation in various industries. Solid mixing has been used in a chemical product manufacturing, food industry, cosmetic industry and pharmaceutical industry. Powder mixing becomes a key process in pharmaceutical manufacturing, especially in solid dosage form processing such as granulation, tableting, and capsule filling. Segregation or de-mixing process is a secondary phenomenon that can occurred after powder homogeneity is reached(3). In batch processing, this phenomenon can be found during handling, during a process such as in hoppers and storage.

Continuous mixing is a process that ingredients are continuously fed and blended in a mixer. During processing, intermediates are sent continuously and directly to the next processing stage. Continuous mixing shows many advantages over batch mixing such as reduce segregation of intermediate, high capacity, less residence time, low hold times between steps and reduce cost(2, 4, 5).

The process requires systems to control and monitor the product quality. Process Analytical Technology (PAT) is a system that provides real-time information for controlling and monitoring processing operations(5). Near-infrared (NIR) spectroscopy is one of the most utilized PAT tools for monitoring continuous mixing. NIRs is a fast and non-destructive analytical technique that can detect multivariable chemical and physical properties. Thus, NIRs is widely used for real-time monitoring of processes(6-8). Other researchers have also used NIRs to develop a quantitative method for monitoring drug content, mixing uniformity and processing stage identification during continuous mixing(7-10).

Most continuous powder mixers are designed as a horizontal cylindrical chamber with screw feeder along its entire length. The screw feeder helps to lift the powder, create motion and movement along the mixer's path resulting in thorough mixing. Segregation may occur resulting from the speed of screw feeder and separation of the mixture into the bottom of the chamber(11).

Vertical mixers utilized in batch processing has not yet been widely used as continuous mixers due to uncontrollable mixing speed and fast flow rate. However, typical vertical mixers, such as vertical screw mixer and vertical ribbon mixer, are found to be able to operate in continuous mode. In addition, vertical mixers offer easier emptying and reduced separation of blended product in the trough.

The purpose of this study is to evaluate the potential of using vertical mixer as a continuous powder mixer and real-time monitoring of the mixing phases using near-infrared spectroscopy as a PAT tool. In this study, model substances are spray dried lactose and iron powder. All materials were mixed with a vertical continuous mixer built in-house. Calibration model was developed for quantitative analysis by NIRs and appropriate chemometrics tools. Impeller alignment and the distance between impellers were varied to investigate the influence of design parameters on the mixing end-point and the concentration of mixture in the steady-state.

Objectives

1. To develop and evaluate continuous powder mixing process using in-house vertical cylindrical mixer
2. To develop calibration model using Near-infrared Spectroscopy (NIRs) as a PAT tool and X-ray powder diffraction (XRPD) as a primary method.
3. To monitor concentrations of mixtures in continuous mixer during steady-state and mixing phases with Near-infrared Spectroscopy (NIRs) after changing impeller alignment and the distance between impellers.



CHAPTER II

LITERATURE REVIEW

1. Pharmaceutical manufacturing

For pharmaceutical industry, pharmaceutical drug products are classified into many dosage forms according to route of administration and physical forms. Most of the medicines are compounded into oral solid dosage. Each dosage form has their own process but occasionally shares the same unit operation. Almost all unit operations in pharmaceutical manufacturing is dominated by batch processing. For oral solid dosage, this product involves many unit operations such as blending, dry granulation, wet granulation, compression and coating. Typical unit operations of oral solid dosage are shown in Figure 2-1.

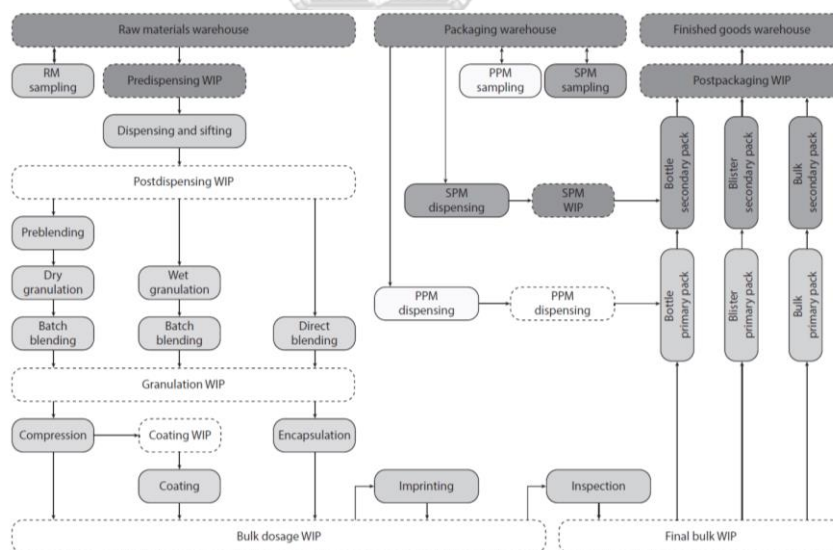


Figure 2-1 Flow diagram of typical oral solid dosage manufacturing(12)

Batch processing

Batch processing is a traditional process that often uses in pharmaceutical production. In this processing, all raw materials in the formula are loaded into the system before starting a process, and all product is released from the system after finishing the processing. Products or intermediates from the process are usually collected and tested off-line as in-process controls for quality checking procedure and stored. When the analytical results are approved, they are transferred to the next step for further processing(5). Batch processing is a less understanding process, time-dependent and less yield when compared with continuous processing(2).

Continuous processing

Continuous processing is an advanced technology that has been gained more interest in pharmaceutical drug manufacturing. This processing is not a new concept. It is a regular processing in many chemical industries. Furthermore, it has been used in the food industry for years by using vertical, gravity-fed processing trains(13). The materials are continuously loaded into, and products are released from the system at the same time entirely the duration of the process. The process is based on a feed rate and time. It typically operates 24 hours a day. There is a system such as a process analytical technology (PAT) for measurement the critical quality parameters. These provide an in-line method and automatically controlling the processing system to ensure that products or intermediates are in the acceptance specification.

Products or intermediates from the process are transfers directly and continuously to the next step. As a result, it can eliminate hold times between steps and intermediate products storage. It offers a great benefit to sensitive materials, intermediates or products that may lead to degradation over time from the environment. This process has the potential to improve product quality, increase efficiency, agility, and robustness of manufacturing. Compared to batch processing, it can enhance production volume by increasing product and process understanding, resulting in reducing out-of-specification material and waste in the manufacturing and reduce batch-to-batch variation. Product scale-up, the bottlenecks of development and launching new drug to market, maybe eliminate or reduce because product and

process development, pilot studies, clinical trials, and commercial manufacturing can use the same equipment. Moreover, it offers economic advantages such as lower cost, less energy consumption, less manufacturing space required, and less labor required (5, 14, 15).

Although continuous processing offers several advantages as described earlier, it still has some challenges and limitations for the adoption this processing in the commercial pharmaceutical manufacturing. This processing comes with a high capital cost of equipment and high technology system to control. Equipment or machines in continuous processing are usually fixed with the product which makes processing stricter. Nevertheless, GEA company has developed a multi-product development and launch rig (DLR) technology connected with process analytical technology which offers plug and play continuous equipment that allows changes between other processing and increase process flexibility(16).

Regulatory issue is one of the challenges that decelerate the change from batch to continuous processing in the pharmaceutical industry(17), especially in the product that is already licensed. This process requires a different method for tracking the quality of product such as time stamps that suitable for real-time release concept. The protocols must be provided when a problem occurs during the flow. Another sample for the challenges is steady-state control. When process is not in steady state, all products during that time has to be quarantined for further analysis and the processing needs to be adjusted to reach steady state again(13). However, regulatory agencies and pharmaceutical companies are finding the solutions for these problematic issues.

Recent years, products from three pharmaceutical companies have been approved for continuous oral dosage manufacturing by the United States Food and Drug Administration (U.S. FDA). Vertex Pharmaceuticals was the first company that U.S. FDA approved their product, Orkambi[®] (lumacaftor/ivacaftor), in July 2015. Followed by a second product, Symdeko[®] (tezacaftor and ivacaftor) approved in February 2018. Both of their medicines were drugs for treating of cystic fibrosis (CF). Their continuous manufacturing process were carried out by GEA continuous processing machine and used intermediate bulk container (IBC) to contain the

materials in each step. The second company that obtained U.S. FDA product approval was Janssen Pharmaceuticals. Their product, Prezista[®] (darunavir), was approved in April 2016 for HIV treatment. Their production line consists of vacuum conveyor to continuously feed powders and to continuous direct compression processing station for automatic tableting and PAT. The third company with U.S. FDA product approval was Eli Lilly. Verzenio (abemaciclib), metastatic breast cancer drug, was approved in September 2017. They used a semi-integrated direct compression continuous processing station that contained powder feeder, blender and tableting station(18).

2. Solid mixing

Solids mixing is one of the essential unit operations in many industries such as chemicals, plastics, food, cosmetics, and pharmaceuticals(19). The goal of mixing is to produce a homogeneous product. Mixture quality depends on many factors such as mixer type, mixer design, mixing time and powder types. Powder mixture can be characterized into three states – perfect or ideal, random and ordered mixture as shown in Figure 2-2. Perfect or ideal mixture is completely uniform mixture that each particle of component identically distributes next to another component. However, this mixture is a zero probability to find in real-life manufacturing. Random mixture and ordered mixture are a mixture that occurs in real commercial manufacturing. A random mixture is a mixture that the probability of finding each particle is equal at every point. An ordered mixture is a concept for cohesive or interacting fine particles when small fine particles attach to surface to one another of coarser particles and form agglomerates(3, 20).

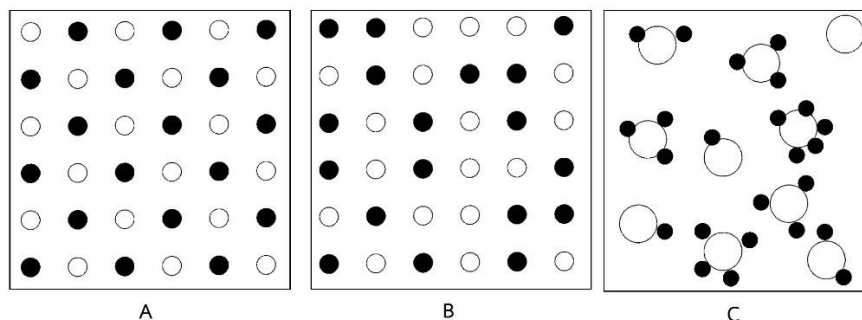


Figure 2-2 States of mixtures.

(A) perfect or ideal mixture (B) random mixture and (C) ordered mixture (19)

There are several factors that affect the quality of the mixture such as component characteristic (particle size, density, etc.), equipment qualification and process condition(21). Segregation or de-mixing is a mechanism that some particles from the blended mixture separate from other components. This problem can happen due to a difference in particle size, particle density, shape, and triboelectric order. Moreover, external mechanical forces such as shear stresses, vibration, and gravity during processing, transfer, and storage can lead to segregation of mixture(19, 20). The example of segregation is shown in Figure 2-3. The segregation problem can be reduced by choosing the mixer and equipment that avoid segregation, add the excipient that increases the flowability of the powder(3).

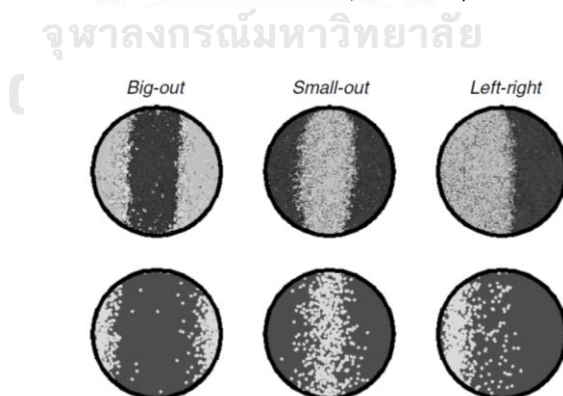


Figure 2-3 Segregation patterns between large (light) and small (dark) grains from top view of a double-cone blender(19).

Batch mixing

All ingredients are charged into a mixer, mixed for a period and discharged when homogeneity is reached as shown in Figure 2-4. The critical parameters that affect the quality of the product are the duration of mixing, the size and type of the mixer, and the operating conditions. Although batch mixing is easier to operate, it has several limits and disadvantages. Segregation is one of the problems that may happen during intermediate transfer and storage(4).

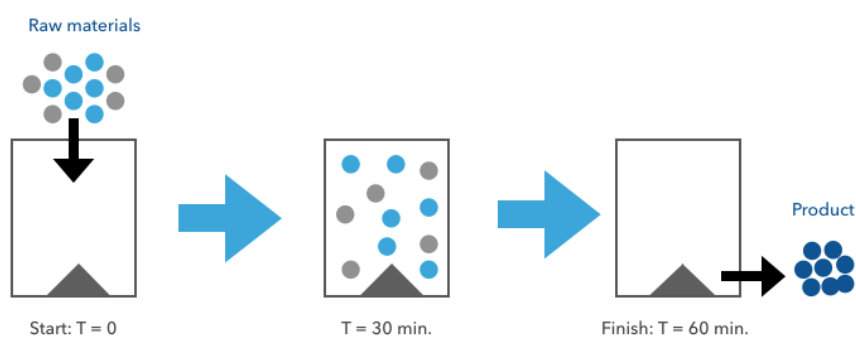


Figure 2-4 Batch processing

From mixing mechanism, batch mixer is divided into two types, tumbler mixer and convective mixers. Most common tumbler mixer used in pharmaceutical mixing unit operations are the double cone, the V-blender, and the bin blender as shown in Figure 2-5. For convective mixer, stirring device inside a mixing vessel create mixing motion and transport materials throughout a vessel. Ribbon blender (Figure 2-6) is one of convective mixer that commonly used in many ranges of mixing processing(19).

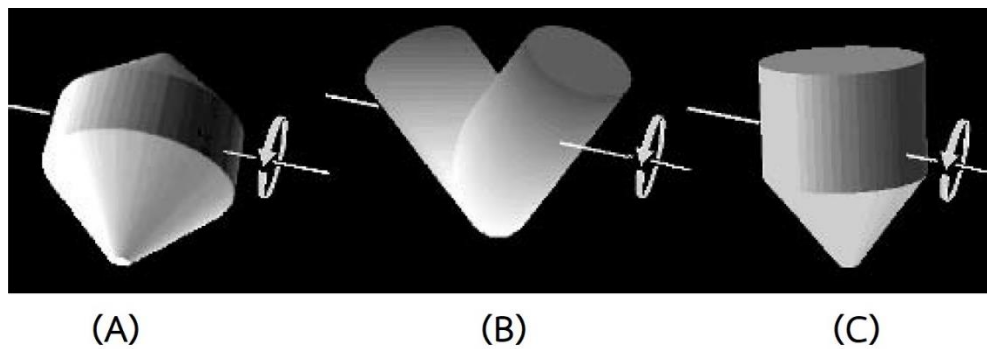


Figure 2-5 Three types of tumbler mixer:
 (A) double cone (B) V-blender (C) bin blender (19).

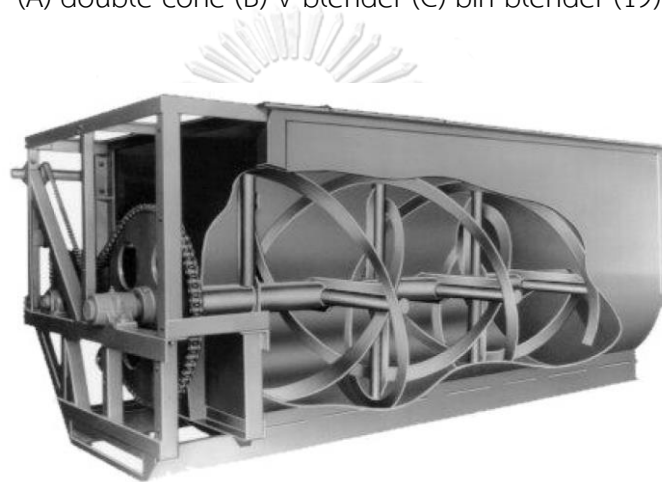


Figure 2-6 Example of convective mixer: ribbon blender(19).

Continuous mixing

For continuous mixing processing, the incoming materials are loaded into the mixer with a constant ratio and rate, and the size of the mixer define the time when the mixture reaches homogeneity as shown in Figure 2-7. This processing is suitable for processing with a high volume of throughput, limited production area, avoiding intermediates storage, and segregation problem. It can minimize segregation by discharge the product close to packaging units

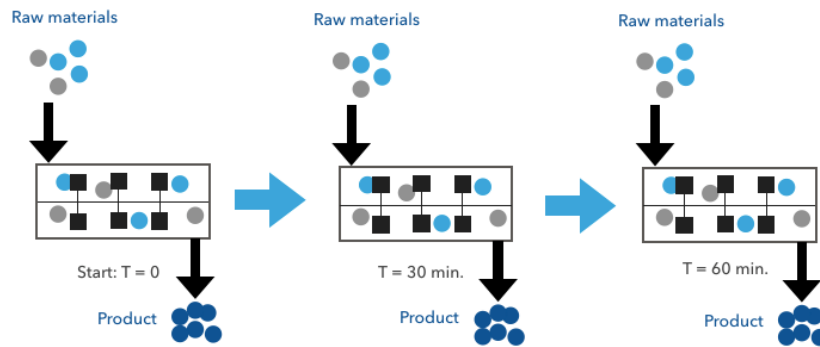


Figure 2-7 Continuous processing.

Continuous mixing offers several advantages over batch mixing as described earlier. Nevertheless, this process still has some limitations. Continuous mixing uses many tools to operate and to monitor the processing. When the equipment is broken, it may affect the processing. All devices especially feeding devices must be regularly calibrated and checked if operate the process within a narrow range.

There are three types of mixer provided for continuous processing – Static mixer, agitated mixer, and tumbling mixer. A static mixer uses two or more simultaneous feeders as a continuous mixing mechanism which is suitable for free-flowing solid. An agitated mixer like ribbon and paddle mixer can be applied for continuous mixing process. These mixers usually load from 30 to 50% full for normal capacity. Rotating drum and zigzag mixer are tumbling mixer that usually uses in continuous mixing process(4). Examples of commercial continuous powder mixer, GCM[®] mixer and Modulomix[®], are shown in Figure 2-8 and Figure 2-9, respectively.

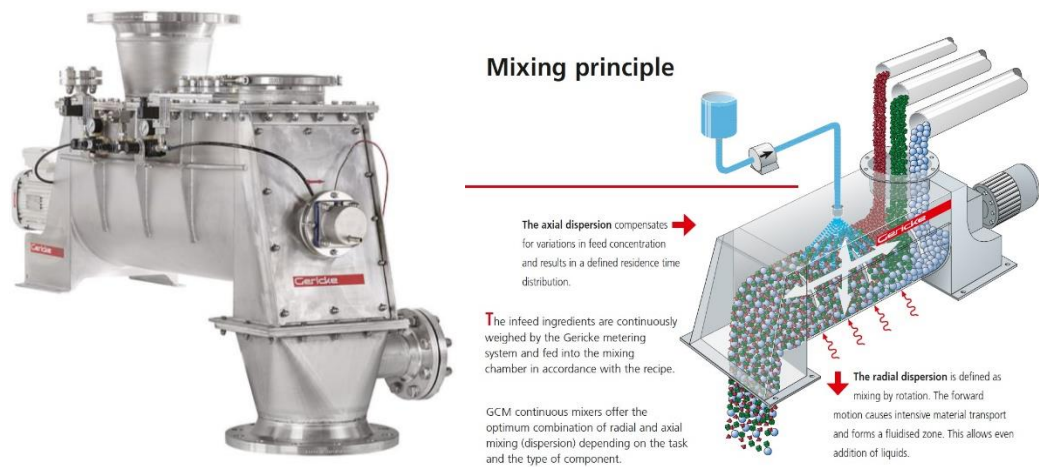


Figure 2-8 GCM continuous mixer from Gericke(22).

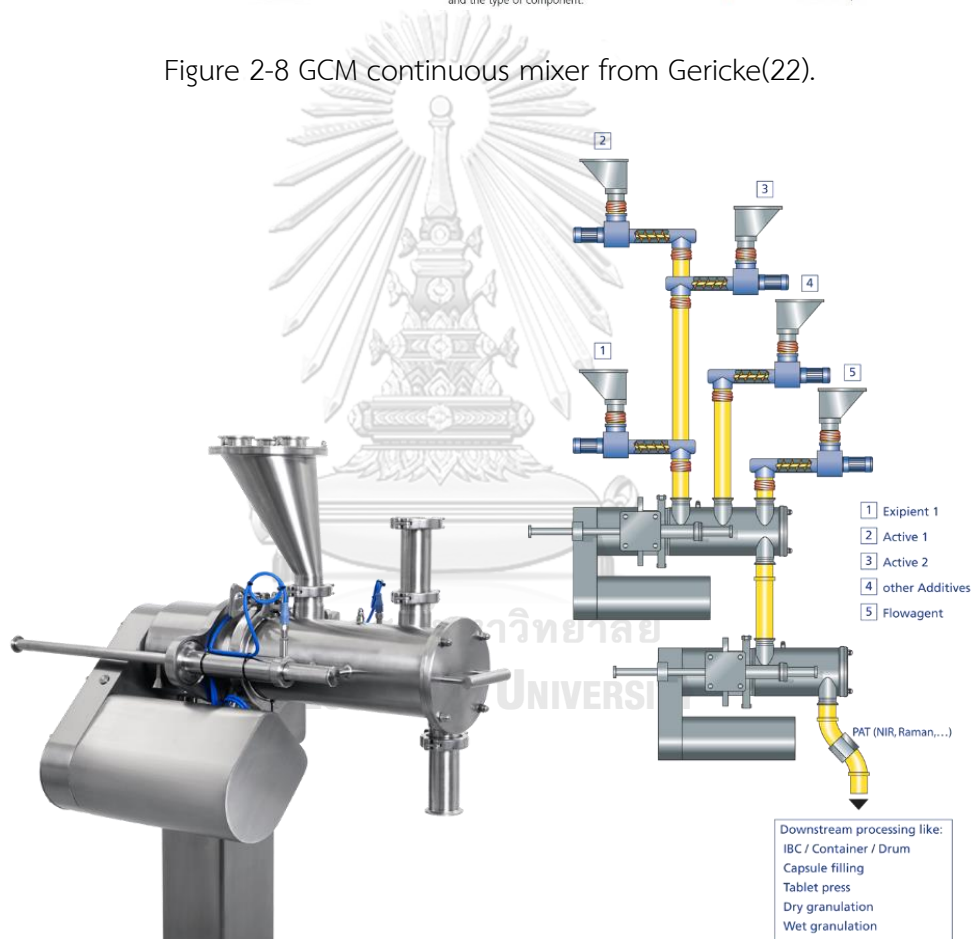


Figure 2-9 Continuous modular mixer (Modulomix) from Hosokawa Micron B.V.(23).

Most of the continuous powder mixer is a horizontal cylindrical chamber that contains a motor-driven impeller inside. Type of impellers that usually used in the mixer is bladed, ribbon, or ribbon-bladed. There are some important parameters that affect the processing (Figure 2-10). The operation parameters consist of a total flow

rate of materials and impeller rotation speed. The design parameters consist of the diameter and length of the mixer which relates to the capacity of the mixer, impeller design (type, number, size, blade angle) and outlet design(11).

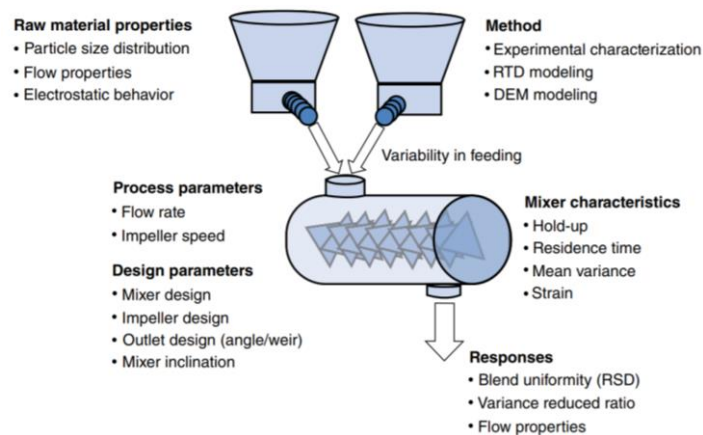


Figure 2-10 Process parameters in continuous powder mixer(11).

The blend homogeneity is one of the critical parameters that relate to the quality of the final product. Homogeneity of blended powder in continuous mixing can justify by present relative standard deviation (%RSD) values obtained by equation 2.1 after the processing has reached a steady state. \bar{C} is the average concentration of the total number of samples (N), C_i is the concentration of each sample and s is the standard deviation which calculated using sample concentrations. With PAT tools, %RSD measurement of continuous mixer offers more reliable estimate due to a larger set of data. The lower %RSD value shows a better mixing(11).

$$\% RSD = \frac{s}{\bar{C}} = \frac{\sqrt{\frac{\sum_1^N (C_i - \bar{C})^2}{N-1}}}{\frac{1}{N} \sum_1^N C_i} \times 100 \quad (2.1)$$

3. Process analytical technology (PAT)

The United States Food and Drug Administration (U.S. FDA) defines process analytical technology (PAT) in pharmaceutical cGMPs for the 21st century as a system for designing, analyzing, and controlling pharmaceutical manufacturing to increase final product quality over a process. Critical quality and performance attributes are set to monitor raw materials, intermediates, and processes. PAT encourages design and quality to be built-into the process. The purpose of PAT is to enhance process understanding, process knowledge and to control the process. PAT tools compose mainly of four components; multivariate tools (for design, data acquisition and analysis), process analyzers, process control tools and continuous improvement and knowledge management tools(24).

Quality and efficiency of a process can be created by using on-, in-, and/or at-line measurements and control to reduce production time, preventing reject or re-processing, promoting real-time release, increasing automation to increase safety and reduce human errors and increasing capacity of processes(25). There are differences between the three sample measurement techniques. A sample is separated from the processing and analyzed near the process stream for at-line measurement, while a sample in on-line measurement is removed for analysis and may be returned to the process stream. A sample is measured in the process stream without removing for in-line measurement, which can be invasive or noninvasive technique.

Near infrared (NIR) spectroscopy

NIR spectroscopy is one of effective PAT tools that has been used for monitoring a critical process and product attributes for real-time measurement during continuous processing. This spectroscopic technique is a quick and non-invasive measurement without sample preparation that provides both qualitative and quantitative analysis.

Characteristic of NIR band

NIR spectrum is a region of the wavelength range of 780 – 2526 nm which relate to the wave number range of 12820 – 3959 nm^{-1} . The overtones and combinations of fundamental vibration of functional groups that contain a hydrogen atom. R-H groups are the strongest NIR absorbers in the NIR region, followed by -CH, -NH, -OH and -SH bond. However, H_2 cannot absorb NIR radiation due to no react of dipole moment between its vibrations(26).

NIR absorption bands are usually broad, overlap with each other, 10 to 100 times weaker than IR bands and band shift caused by a hydrogen bond. NIR is available in various measuring modes such as transmittance, diffuse reflectance, and transfectance, depending on the optical properties of the sample. Transmittance is usually for measuring transparent materials. Diffuse transmittance, diffuse reflectance, transfectance are usually for measuring turbid liquids, semi-solids, and solids which rely on the absorption and scattering characteristic of the material. For solid samples, a density of packed powder or position of tablets or capsules sample may cause spectra error by scattering effect and stray light(27).

Pretreatment

NIR spectra usually contain unfavorable spectral variations and baseline shift from various reasons. For example, solid samples or turbid liquids can cause light scattering. Pathlength variations cause poor NIR spectra. physical properties of sample, particle size and density, and temperature can cause variation. An instrumental effect from a detector, an amplifier and an AD converter can cause random noise. To remove or reduce this effect, NIR spectral data should apply pretreatment before spectra used to improve the quality of data(28).

Pretreatment technique can be classified into two groups: scatter correction methods and spectral derivatives. Both techniques are widely applied for NIR spectral pretreatment. Scatter correction methods consist of multiplicative scatter correction (MSC), inverse MSC, extended MSC (EMSC), extended inverse MSC,

de-trending, standard normal variate (SNV) and normalization. Spectral derivatives consist of Norris-Williams (NW) derivatives and Savitzky-Golay (SG) polynomial derivative filters. Moving average and Savitzky-Golay method are for smoothing the spectra and noise reduction. Derivative, MSC, and SNV are for baseline correction. Overlapping bands can improve resolution by using derivatives. The technique that mostly used for NIR pretreatment is MSC, SNV, and spectral derivative, respectively.

Multiplicative scatter correction (MSC) is a method for correcting baseline vertical variations and baseline inclination. The correction of MSC uses a simple linear univariate to fit with a standard spectrum which is consists of two steps. The first step is the correction coefficients estimation (additive and multiplicative contributions) as equation 2.2. The second step is the recorded spectrum correction as equation 2.3

$$X_{\text{org}} = b_0 + b_{\text{ref},1} \cdot X_{\text{ref}} + e \quad (2.2)$$

$$X_{\text{corr}} = \frac{X_{\text{org}} - b_0}{b_{\text{ref},1}} = X_{\text{ref}} + \frac{e}{b_{\text{ref},1}} \quad (2.3)$$

Where,

X_{org}	=	an original sample NIR spectra
X_{ref}	=	a reference spectrum for pretreatment the entire dataset
e	=	the un-modeled part of X_{org}
X_{corr}	=	the corrected spectra
b_0	=	the offset correction
$b_{\text{ref},1}$	=	the correction according the i^{th} order of the reference

Standard Normal Variate (SNV) is the second most applied technique. SNV does not need the reference spectrum which differs from MSC. Nevertheless, MSC and SNV show the same result for most of the practical applications. The calculation of SNV is followed by equation 2.4.

$$X_{\text{corr}} = \frac{X_{\text{org}} - a_0}{a_1} \quad (2.4)$$

Where,

X_{org}	=	an original sample NIR spectra
X_{corr}	=	the corrected spectra
a_0	=	the average value of the sample spectra after corrected
a_1	=	the standard deviation of the sample spectra (X_{org})

A spectral derivative is a method for enhancing the resolution of spectra and baseline correction. This method can remove spectra additive and multiplicative effect. The first-order derivative removes baseline. The second-order derivative, the most used, removes both linear trend and baseline. The spectral derivative has two methods: Norris-Williams derivation (or gap derivation) and Savitzky-Golay derivation.

Norris-Williams derivation is a method that avoids noise inflation. This method starts with smoothing the spectra to reduce the signal-to-noise ratio followed by first-order or second-order derivation. The gap in this method is usually used, when the data has a frequency component. This value relates to the distance between two peaks values in the signal.

Savitzky-Golay derivation is a widespread method for vector derivation with smoothing method. The raw data will fit a polynomial in a symmetric window to estimate the derivative at a center point. The value that used for estimate derivative for center point obtains by calculated the parameters for the polynomial such as the number of points for calculating the polynomial (window size) and the degree of the fitted polynomial.

The Norris-Williams derivation and Savitzky-Golay derivation normally provide difference estimate. Moreover, the number of points lost is different in calculation between Norris-Williams derivation and Savitzky-Golay derivation. Norris-Williams derivation is the number of points used for smoothing plus the size of the gap minus one, while Savitzky-Golay derivation is the number of points used for smoothing minus

one. Norris-Williams derivation can absorb more points than Savitzky-Golay derivation, so wavelengths can be lost which importance in short spectra(29).

Quantitative analysis by multivariate calibration

Chemometric is a method that extracts information from the chemical and physical data by using statistic and mathematics. The data, obtained from NIR, must be treated by using multivariate calibration which is one of the chemometric method before qualitative analysis. The calibration process can be done by selecting a calibration sample set, define reference values, set the spectral variations to the reference value, and finally validate the model.

Principal component regression (PCR) and partial least-squares (PLS) regression are the multivariate technique that most often used in quantitative analysis. PCR performs regression on the sample by using the principal component analysis (PCA). PCR uses only the major components in x-variables which is not related to y-variables and shows only the variations in the spectrum. Accordingly, PLS regression is built to solve this problem(30). PLS uses both spectral variables and respective parameter variables information which represents the most relevant variations. PLS creates a linear link between the spectral data (X) and the reference values (Y) in the matrices and calculates with least squares algorithms(31).

Validation is the next step after creating the calibration equation for evaluating the performance of the calibration model. The reliability of the model should be considered with the root mean square error (RMSE). Root mean square error of calibration (RMSEC) estimates prediction error of the reference values in the calibration data set as an internal validation. This value estimates error more than prediction error of the model. Root mean square error of prediction (RMSEP) estimates the variation of the reference and predicted values in an independent validation set. This value is more reliable for prediction error than internal validation. The coefficient of determination (R^2) determines the quality of a model. R^2 which closely to 1.0 is the

most required for calibration model(32). The most desire calibration model should have the highest R^2 with the lowest of RMSEC and RMSEP.

4. Implementing NIRs in continuous mixing process

NIR spectroscopy has been applied for monitoring continuous mixing process by the horizontal continuous mixer in many studies. Most of the studies have developed a multivariate calibration model using PLS regression model for real-time drug concentration monitoring.

Vanarase et al. (8) used the continuous blender (Gericke model GCM-250) for the continuous mixing process. They developed a multivariate calibration model using PLS regression model for real-time monitoring the concentration of acetaminophen with in-line wireless NIR spectrometer at an outlet of the blender.

In the following paper of Vanarase et al. (33), they studied the effect of process parameters on blend homogeneity in the same continuous powder blender. Two blade configurations had been used in this study, all forward and alternate. The results showed that the rotation rate was the most critical process parameters which affected mixing performance. The blade configuration also affected the blend homogeneity with statistically significant. The results indicated that alternate blade configuration showed better mixing performance in both low and high flow rate. Consequently, the intermediate rotation rate and alternate blade configuration showed the best mixing performance with the lowest RSD.

Järvinen et al. (10) used in-line NIR spectroscopy (VisionNIR Is) for determining acetaminophen content of powder mixtures and tablets. They used KM5, provided by Gebrüder Lödige Maschinenbau GmbH, as a continuous mixing line and followed by rotary tablet press for direct compression tableting process. They developed a multivariate analysis using PLS regression model with the Unscrambler software. The spectra results were compared to UV-visible spectroscopy as an off-line reference method.

Martínez et al. (7) used in-line NIR probe to quantify the API content in the mixture from the continuous blender, Modulomix technology by Hosakawa Micron. The purpose of the study was to develop a chemometric analysis by using PLS regression model, to identify the phase present during the continuous mixing process: start-up, steady stage, and emptying using PCA. The results showed that PLS could be applied for continuous mixing process monitoring. Furthermore, PCA, MBSD, and RSD could be used as qualitative tools for phase determination.

Portillo et. al. (34) studied the effect of mixing angle, rotation rate, and cohesion to the homogeneity of the mixture. Continuous mixer manufactured by GEA Buck Systems. They used TQ Analyst program and built a model using PLS regression. The homogeneity of samples at an outlet was calculated using the relative standard deviation (RSD). The results showed that the mixing angle was the most significant factor that effects on homogeneity, followed by rotation rate. However, cohesion did not play a significant role in homogeneity.

Furthermore, the effects of processing parameters had been investigated in Osorio and Muzzio (35) study. They studied the effects of rotational speed and flow rate (processing parameter) and blade pattern (type and configuration) on a new continuous powder mixer, GCG-70 by Glatt®. The blended powder was collected at the outlet of the mixer at different time intervals for the residence time distribution. The samples were analyzed by FT-NIR spectrometer and used PLS as a regression method for blend uniformity measurement. The results indicated that Impeller rotation speed showed inverse results to the hold-up and the mean residence time. These values decreased when impeller rotation speed increased. However, the mean centered variance and the number of blades pass showed a similar result. When impeller rotation speed increased, these values also increased. For flow rate, the hold-up showed inverse results, but the mean residence time and the number of blades pass showed a similar result. Blade pattern affected the mixing dynamics when the rotation rate increased.

5. Direct compressible excipients

Directly compressible excipients are inactive pharmaceutical excipients that have been used for improving flowability during direct compression tableting process. Spray dried lactose (Flowlac[®] 100) is a mixture of amorphous lactose which is a white to off-white crystalline particles or powder. Flowlac[®] 100 from Meggle exhibits spherical agglomerate shape with particle size of approximately 200 μm , as shown in Figure 2-11.

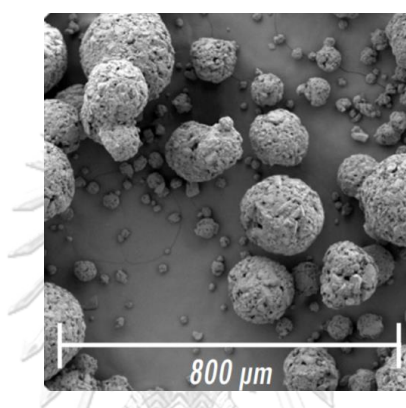


Figure 2-11 SEM photomicrograph of spray dried lactose (Flowlac[®] 100)(36).

Pregelatinized starch is a white to off-white powder with a moderately coarse to fine. It is a starch that has been processed by breaking all or some part of starch granule's structure with chemical and/or mechanical method. Starch 1500[®] from Colorcon[®] shows irregular shape with average particle size of approximately 65 μm , as shown in Figure 2-12.

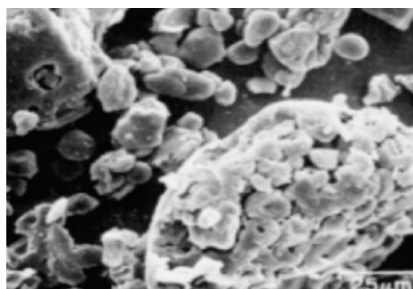


Figure 2-12 SEM photomicrograph of Pregelatinized starch (Starch 1500[®])(37).

Microcrystalline cellulose (MCC) is a white powder composed of porous particles. It is a cellulose that has been purified and partially depolymerized. MCC is commercially available in various grades with different particle sizes and moisture properties. For PH 102, it is a grade of MCC that is widely used in direct compression tableting process. CEOLUS[®] PH 102 from Asahi Kasei Chemicals Corporation has a uniform fibrous shape with larger particle size of approximately 90 μm , as seen in Figure 2-13.

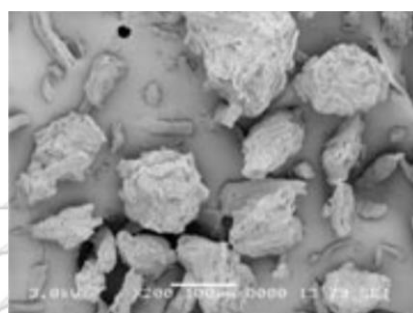


Figure 2-13 SEM photomicrograph of microcrystalline cellulose PH 102 (CEOLUS[®] PH 102)(38).

CHAPTER III

MATERIALS AND METHOD

Materials

- Iron powder (Suksapanpanit, Thailand)
- Spray dried lactose (FlowLac[®] 100, Meggle, Wasserburg, Germany)
- Pregelatinized starch (Starch 1500[®], Colorcon[®], United States)
- Microcrystalline cellulose PH 102 (CEOLUS[®] PH 102, Asahi Kasei Chemicals Corporation, Japan)

Equipment

- Fourier transformed near-infrared spectrometer (Antaris[™] II FT-NIR analyzer, Thermo Scientific[™], Wisconsin, USA) with diffuse reflectance fiber-optic probe (SabIR[™] probe, Thermo Scientific[™], Wisconsin, USA)
- Powder X-ray Diffractometer (MiniFlex[™] II, Rigaku, Tokyo, Japan)
- Tapped density tester (in-house model)

Method

1. Material selection

Flowability of materials was evaluated in this experiment. Free flowing materials were the most desired. Direct compressible excipients, spray dried lactose (Flowlac[®] 100), pregelatinized starch (Starch 1500[®]) and microcrystalline cellulose PH-102 (CEOLUS[®] PH-102) were selected. Flowability was evaluated by means of obtaining appropriate Hausner Ratio in equation 1. Best flowability is shown by values obtained are close to 1. The excipient that showed the best results in Hausner Ratio

would be selected for the continuous mixing process. Furthermore, another material for the process was iron powder. It was chosen as model ingredient in this experiment because it was a free-flowing material with reusable properties.

$$\textit{Hausner Ratio} = \frac{V_o}{V_t} \quad (1)$$

Where,

V_o = unsettled apparent volume

V_t = final tapped volume

2. Vertical continuous powder mixer

2.1. Structure

The continuous powder mixing machine was designed for vertical powder mixing. The machine composed of 6 parts: glass mixing chamber, mixing impellers, shaft, hoppers, motor and body (Figure 3-1). Mixing chamber was a vertical cylindrical shape glass with a slope at the outlet of the chamber. Three blades mixing impellers, made from 315 stainless steel, were used which were able to be adjusted in both direction and position. These impellers were mounted on a vertical rotating shaft. Two hoppers were made from two plastic bottles with ball valves to control the feed rate of incoming materials.

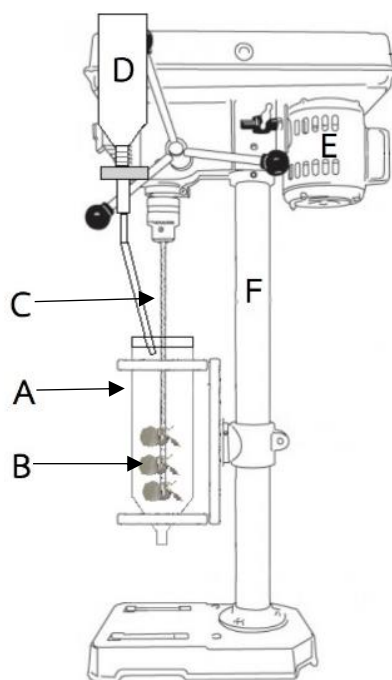


Figure 3-1 Machine structure.

(A) mixing chamber (B) mixing impellers (C) shaft (D) hoppers (E) motor (F) body

2.2. Vertical continuous powder mixer operating principles

After the machine was turned-on, materials freely flowed into the mixing chamber with a constant rate controlled by ball valve. Impellers that attached on the vertical rotating shaft would rotate and mixed all materials together and passed them to an outlet at the end of the chamber. The flowrate of output was controlled by ball valve.

3. NIR calibration model development

All static samples were measured by NIR for calibration model development. NIR was used to determine spray dried lactose contents in the formula and X-ray powder diffraction (XRPD) analysis was used as reference values. NIR diffused reflectance fiber-optic probe was attached at a wall of a mixing chamber while placed in horizontal position (Figure 3-2). NIR spectra were collected via RESULT™ software provided by Thermo Scientific™. Each spectrum was programmed to collect average of 32 scans and 32 cm^{-1} resolution with a range of 4000-10000 cm^{-1} .

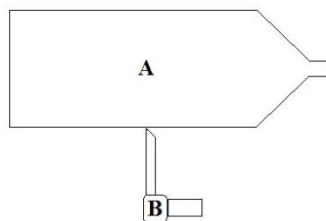


Figure 3-2 Experimental setup for obtaining NIR calibration model.

(A) mixing chamber (B) NIR fiber optic probe

3.1. Preparation of calibration samples

For NIR calibration model development, Iron powder and spray dried lactose physical mixtures were prepared in seven concentrations ranging from 20% to 100% (w/w) of spray dried lactose. All calibration samples were weighed approximately 20 g and mixed until homogeneity was reached. Total of 20 NIR spectra for each concentration was collected for calibration model.

3.2. XRPD analysis

Off-line XRPD analysis was used as the reference method to confirm the prediction of the NIR calibration model. Data were obtained within the 2θ range of 15 to 25 $^{\circ}2\theta$ with a step size of 0.02 degree (MiniFlex™ II, Rigaku). The average absorbance of pure iron powder was used for baseline correction for physical mixtures.

3.3. NIR data processing

Total of 140 spectra were divided into two groups, 77 spectra for calibration set and 63 spectra for the validation set. The spectra obtained were evaluated by Unscrambler X 10.4. NIR spectra needs reference value to indicate the value for each spectrum. XRPD intensity at dominant peak of spray dried lactose at 20 $^{\circ}2\theta$, calculated from the previous calibration curve of XRPD, was used by Unscrambler program for creating NIR calibration model.

To find the suitable model, the raw NIR spectra were applied for the eligible wavelength regions and pretreatment methods. Wavelength regions selected corresponded to iron powder peak and spray dried lactose level variations.

Four spectral ranges, 4000 – 10000, 4000 – 6000, 4000 – 7600 and 6800 – 8700 cm^{-1} , were selected for initial model evaluation. After the best range was chosen, the selected spectral range was pretreated with methods shown in Table 3-1. The spectral pretreatment was performed with multiplicative scatter correction (MSC) and standard normal variate (SNV) follow by first and second derivative operations obtained by Norris-Williams or Savitzky-Golay smoothing algorithms.

Table 3-1 Pretreatment methods for NIR spectra.

No.	First step		Second step	
	Multiplicative Scatter Correction (MSC)	Standard Normal Variate (SNV)	Derivative	Smoothing
1	-	-	-	-
2	-	-	1 st	Norris-Williams
3	-	-	1 st	Savitzky-Golay
4	-	-	2 nd	Norris-Williams
5	-	-	2 nd	Savitzky-Golay
6	✓	-	-	-
7	-	✓	-	-
8	✓	-	1 st	Norris-Williams
9	✓	-	1 st	Savitzky-Golay
10	✓	-	2 nd	Norris-Williams
11	✓	-	2 nd	Savitzky-Golay
12	-	✓	1 st	Norris-Williams
13	-	✓	1 st	Savitzky-Golay
14	-	✓	2 nd	Norris-Williams
15	-	✓	2 nd	Savitzky-Golay

Partial least squares (PLS) algorithm was used to develop NIR calibration model after the spectra were pretreated. The calibration model's performance was evaluated in terms of root mean standard error for calibration (RMSEC), root mean standard error for prediction (RMSEP) and correlation coefficient (R^2).

4. Real-time continuous mixing process monitoring, data processing and analysis

4.1. Set-up for real-time continuous mixing process monitoring

To obtain the spectra in real-time process monitoring, NIR diffused reflectance fiber-optic probe was placed close to the wall of the glass mixing chamber along the vertical axis as shown in Figure 3-3.

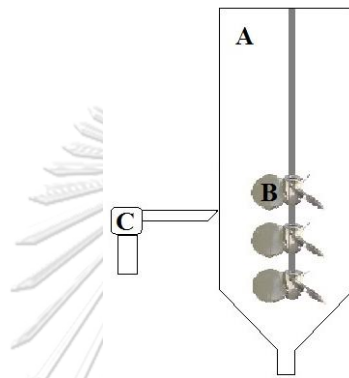


Figure 3-3 Experimental setup for monitoring continuous powder mixing process.

(A) mixing chamber (B) propellers (C) NIR fiber optic probe

In this study, three mixing impellers were installed 14 cm away from an outlet (L) according to Figure 3-4. The chamber was filled with spray dried lactose over mixing impeller no. 1 (H) up to 1.50 cm before starting the process. Materials were mixed at a constant rate of approximately 145 rpm which controlled by a motor. Spray dried lactose and iron powder feed rate were kept constant at 2.0 g/s and 0.5 g/s, respectively. The total material inlet feed rate was associated with constant outlet rate of 2.5 g/s. In each trial, the materials were prepared for two minutes flow duration. The target concentration was set at 80% w/w of spray dried lactose and 20% w/w of iron powder. NIR spectra were obtained immediately after materials were introduced through the mixing chamber. Two positions of NIR fiber-optic probe was placed between mixing impellers (probe no.1 and no.2) with distances between impellers (I) of 0.5 and 1.0 inch as shown in Figure 3-4.

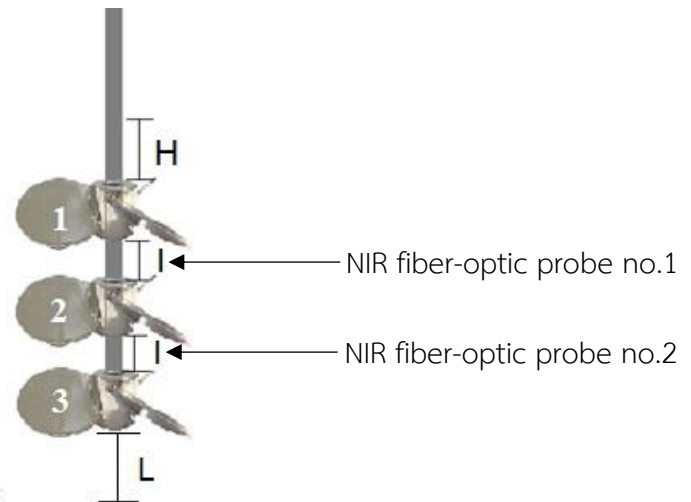


























Figure 3-4 Mixing impeller configurations and NIR fiber-optic probe positions.

(H) spray dried lactose level over mixing impeller no. 1 before starting the experiment (I) distance between impellers and (L) distance of mixing impellers no.3 installed away from outlet

In order to study the effect of continuous powder mixing on steady-state determination, distances between each mixing impeller and configuration of mixing impellers were varied. The distances between the mixing impellers (I) were 0.5 and 1.0 inch. This distance was set between mixing impellers no.1 and no.2. The configuration of mixing impeller was adjusted into two alignments, aligned and opposite directions. Only mixing impeller no.2 was rotated 90 degrees for opposite direction, while no.1 and no.3 were fixed. The mixing impeller settings are shown in Table 3-2. In addition, the mixtures were collected every one minute from the outlet since the process began until finished for off-line NIR analysis to determine the final concentration of the mixtures.

Table 3-2 Mixing impeller set-up for each trial.

Trial	Probe NIR position	Distance between impellers (l)	Mixing impeller			
			alignment	No. 1	No. 2	No. 3
A	1	0.5	Aligned			
B	2	0.5	Aligned			
C	1	0.5	Opposite			
D	2	0.5	Opposite			
E	1	1.0	Aligned			
F	2	1.0	Aligned			
G	1	1.0	Opposite			
H	2	1.0	Opposite			

4.2. NIR spectral measurements

NIR spectra for real-time process monitoring were obtained by Fourier transformed near-infrared spectrometer (Antaris™ II FT-NIR analyzer) with a diffuse reflectance fiber-optic probe designed for in-line analysis. The spectra were obtained with an average of 2 number of scans and 32 cm^{-1} resolution with a scanning range of $4000\text{-}10000\text{ cm}^{-1}$.

4.3. Data processing and analysis

NIR data obtained from NIR diffused reflectance fiber-optic probe were processed using Unscrambler® X 10.4. Previously developed NIR calibration model was used for data analysis. The raw data from real-time processing had been corrected by the average concentration of spray dried lactose, which obtained after the mixing machine was turned-on. After baseline correction, data were plotted using scattered plots for phase determination. Moreover, homogeneity of the mixtures was evaluated by percent relative standard deviation (%RSD) which was calculated for each moving block of ten consecutive concentrations. The average predicted NIR concentration of real-time measurement and mixtures collected from outlet during steady-state were calculated and were statistically compared using one-way ANOVA by Minitab program.

CHAPTER VI

RESULTS AND DISCUSSIONS

1. Materials selection

Model substances in this experiment were chosen from directly compressible excipients and iron powder (Figure 4-1). Each directly compressible excipient shows differences in shape which effect its flowability. Spray dried lactose (FlowLac[®] 100) shows spherical agglomerate shape (Figure 2-11), pregelatinized starch (Starch 1500[®]) shows irregular shape (Figure 2-12) and microcrystalline cellulose PH 102 (CEOLUS[®] PH 102) shows uniform fibrous shape (Figure 2-13).

Reasons of choosing iron powder as one of model substances in this experiment were due to the vertical continuous mixer needed good flowability of materials and the lack of gravimetric hopper to weigh materials and use screw feeder to pass materials forward. Iron powder was selected due to it is a free-flowing material which was possible to control flow rate by ball valve. In addition, iron powder had different color from directly compressible excipients which led to an ease to monitor during mixing process.



Figure 4-1 Iron powder used in the experiment

Particle size distribution of iron powder obtained from sieve analysis was shown in Figure 4-2. Most of iron powder was 0.18 mm.

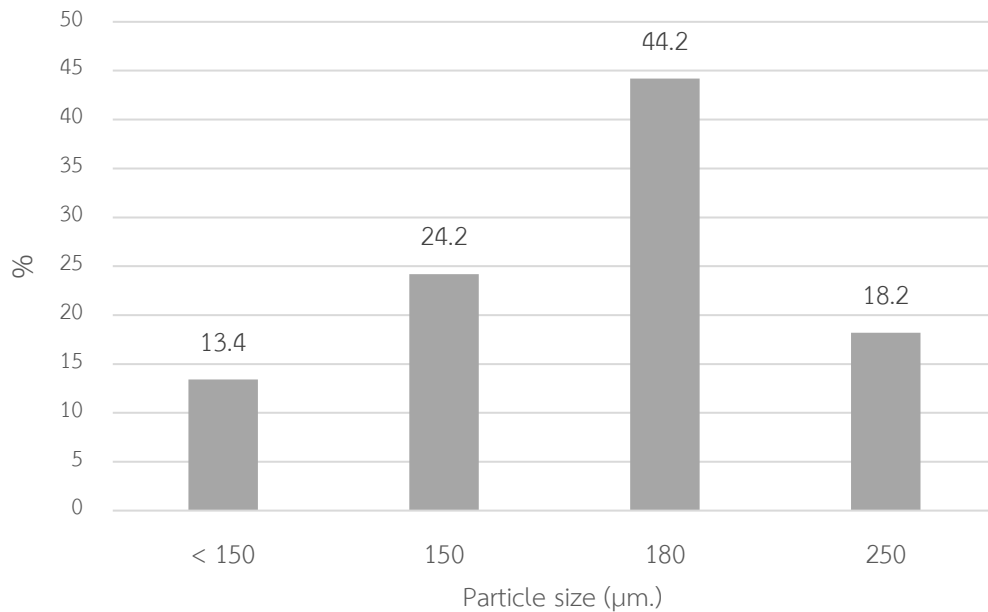


Figure 4-2 Particle size distribution of iron powder.

Hausner ratio was selected for predicting material flow characteristic, which was determined by measuring unsettled apparent volume (V_o) and final tapped volume (V_t) in a graduated cylinder of 20 ml. Hausner ratio and flow character of the materials are shown in Figure 4-3.

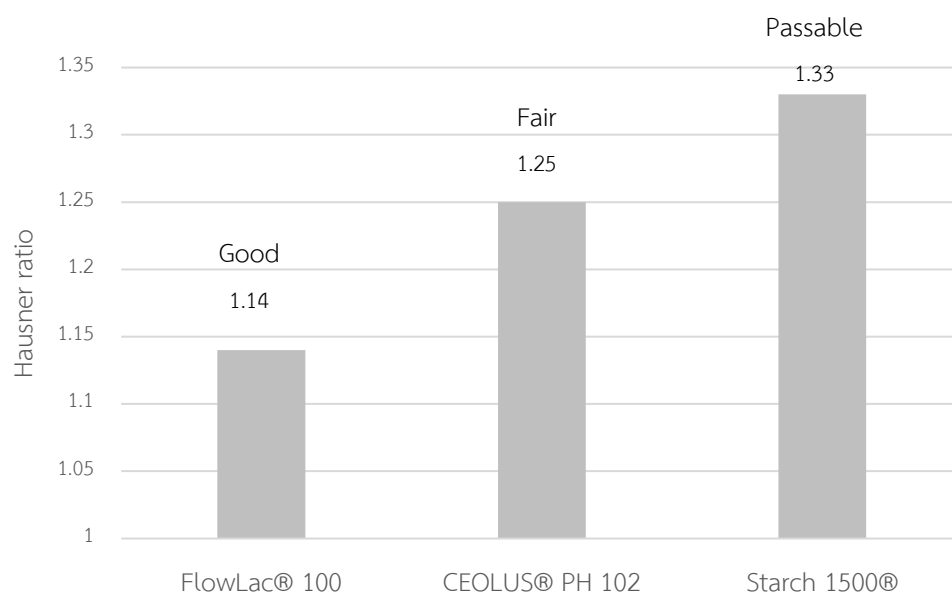


Figure 4-3 Hausner ratios and flow characters of directly compressible excipients.

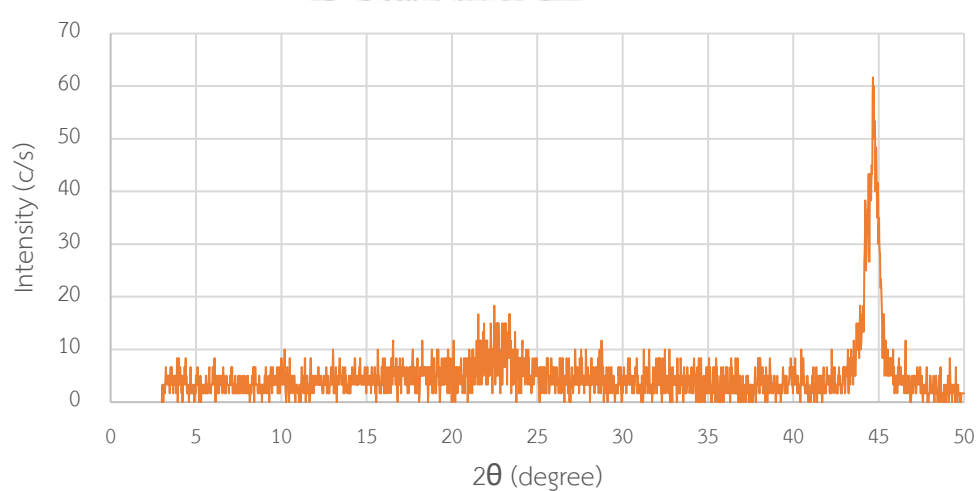
Hausner ratio of spray dried lactose (FlowLac® 100), microcrystalline cellulose PH 102 (CEOLUS® PH 102) and pregelatinized starch (Starch 1500®) are 1.14, 1.25 and 1.33, respectively. Material with the least Hausner ratio showed better flow character. Spray dried lactose showed the best flow character (good) among all three materials followed by microcrystalline cellulose PH 102 and pregelatinized starch with passable and fair flow characters, respectively. Consequently, Spray dried lactose was selected as an excipient in the continuous mixing process.

2. NIR calibration model development

2.1. XRPD analysis

Iron powder (Figure 4-4), spray dried lactose (Figure 4-5) and known mixtures (Figure 4-6) were selected for creating XRPD calibration curve used as a reference method for future NIR study. This calibration curve will be used to predict concentrations of spray dried lactose in the static and dynamic (continuous) unknown mixtures. In this experiment, the target concentration of final mixtures was set at 80 %w/w. Each concentration was measured with XRPD in triplicates. The linearity of the study resulted in correlation coefficient (R^2) of 0.974 at peak position $20^\circ 2\theta$ as shown in Figure 4-7.

From the calibration curve of XRPD analysis in Figure 4-7, it could be observed that the ratio of iron powder in the spray dried lactose/iron powder mixtures affected XRPD analysis results. Peak position at $20^\circ 2\theta$ shows dominant character of spray dried lactose more than iron powder. Mixtures with high concentration of spray dried lactose of more than 60 %w/w are shown to be more linear and obeyed the correlation trendline and also can be observed in NIR spectra of Figure 4-9. This may be due to the high concentration of iron powder in the physical mixtures of more than 40 %w/w changed the reflection of XRPD which affected the intensity of mixtures. Thus, mixtures with lower concentrations of spray dried lactose, 20 and 40 %w/w, were curvilinear (Figure 4-7).



CHULALONGKORN UNIVERSITY
Figure 4-4 XRPD diffraction pattern of iron powder

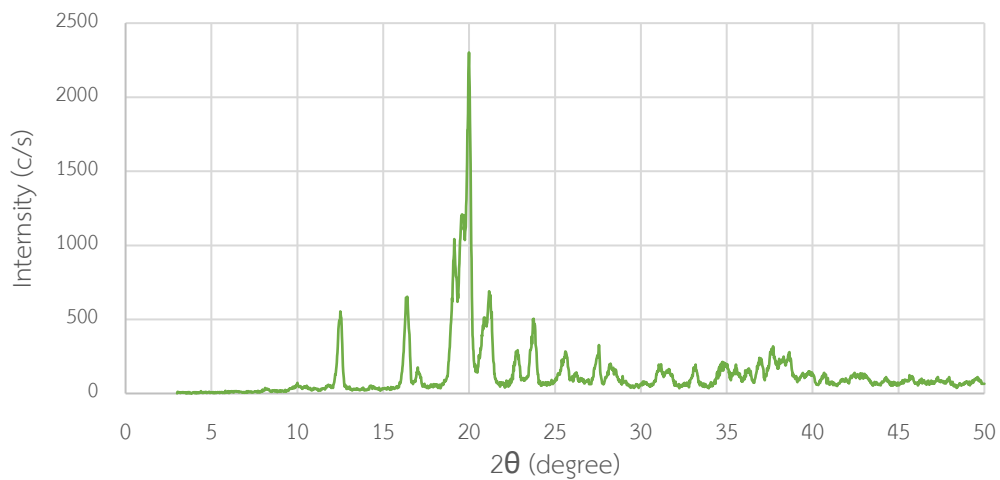


Figure 4-5 XRPD diffraction pattern of spray dried lactose (FlowLac® 100).

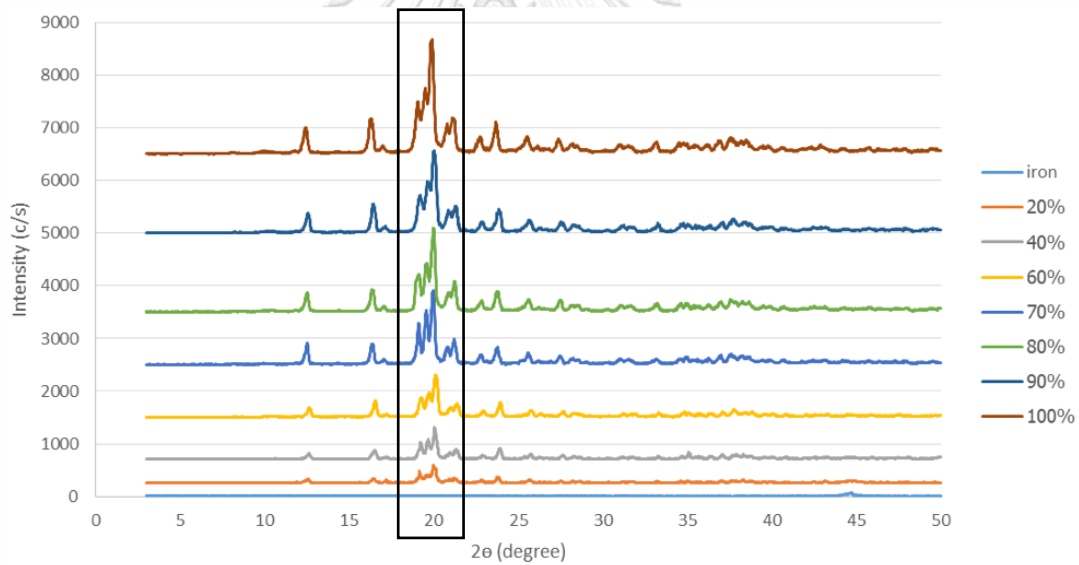


Figure 4-6 XRPD diffraction patterns of spray dried lactose in iron powder physical mixtures of known concentrations.

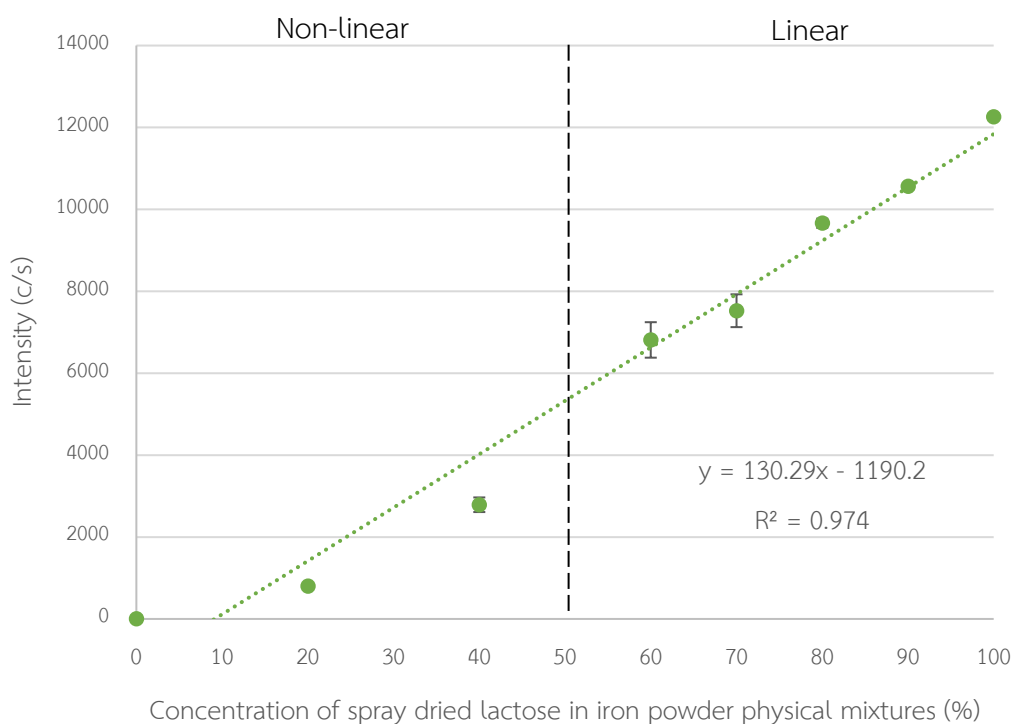


Figure 4-7 Calibration curve of XRPD intensity at 20 °2 θ and concentrations of spray dried lactose in spray dried lactose/iron powder physical mixtures.

2.2. NIR calibration model development

The static NIR spectra of pure iron powder, spray dried lactose and known mixtures were measured and are shown in Figure 4-8. Iron powder shows two distinct absorption bands at 4518 and 7139 cm^{-1} (Figure 4-8 (A)). Spray dried lactose shows spectral characteristic as seen in Figure 4-8 (B).

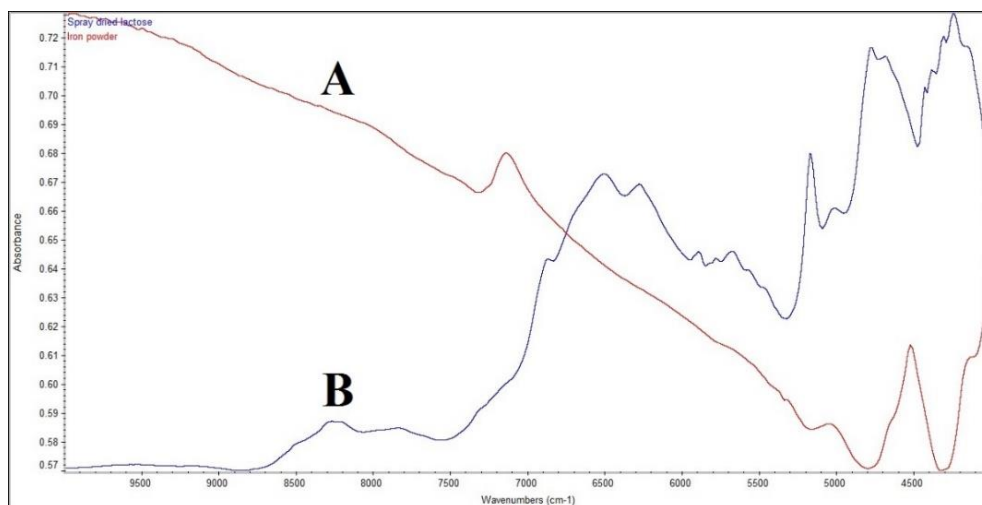


Figure 4-8 NIR spectra of pure iron powder (A) and spray dried lactose (B)

The changes in spray dried lactose concentrations were observed to be correlated to decreasing spray dried lactose amounts in iron powder as shown in Figure 4-9. As can be observed that high lactose concentrations can be differentiated from low concentrations of less than 40 %w/w similar to the results obtained by XRPD for constructing calibration curve.

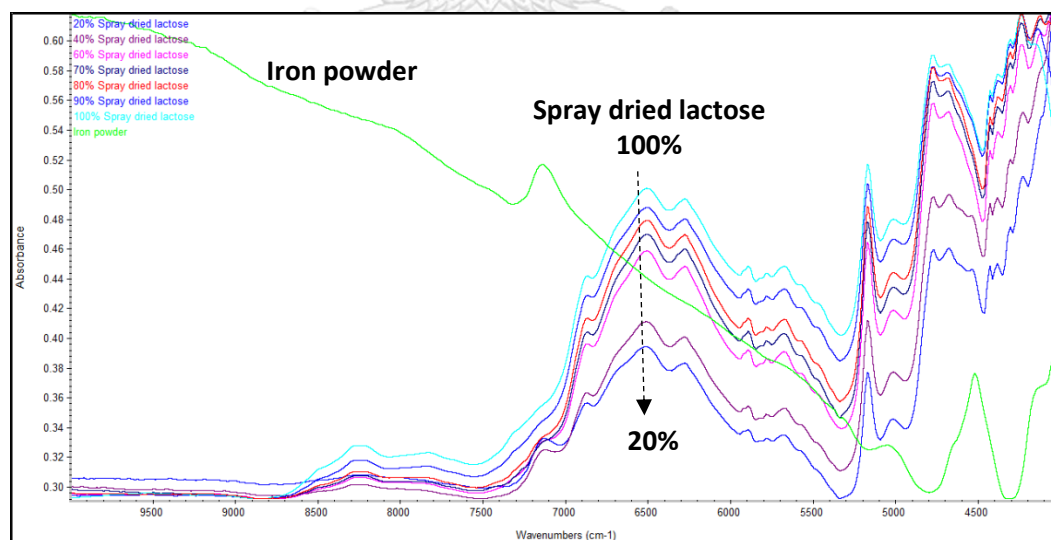


Figure 4-9 NIR spectra of iron powder, spray dried lactose and 20% to 90% (w/w) spray dried lactose/iron powder physical mixtures.

Four wavenumber ranges relating to spray dried lactose and iron powder were selected for comparisons: 4000 – 10000, 4000 – 6000, 4000 – 7600 and 6800 – 8700 cm^{-1} . Each range represents different characteristic peaks of each materials. Range between 4000 – 10000 cm^{-1} was considered as a full NIR range which represented both iron powder and spray dried lactose. While 4000 – 6000 cm^{-1} represents one iron powder at 4518 cm^{-1} . 4000 – 7600 cm^{-1} indicates both iron powder peaks at 4518 and 7139 cm^{-1} . Lastly, 6800 – 8700 cm^{-1} indicates one iron powder peak at 7139 cm^{-1} . Figure 4-10 to Figure 4-13 show NIR calibration model for each of the four wavenumber ranges.

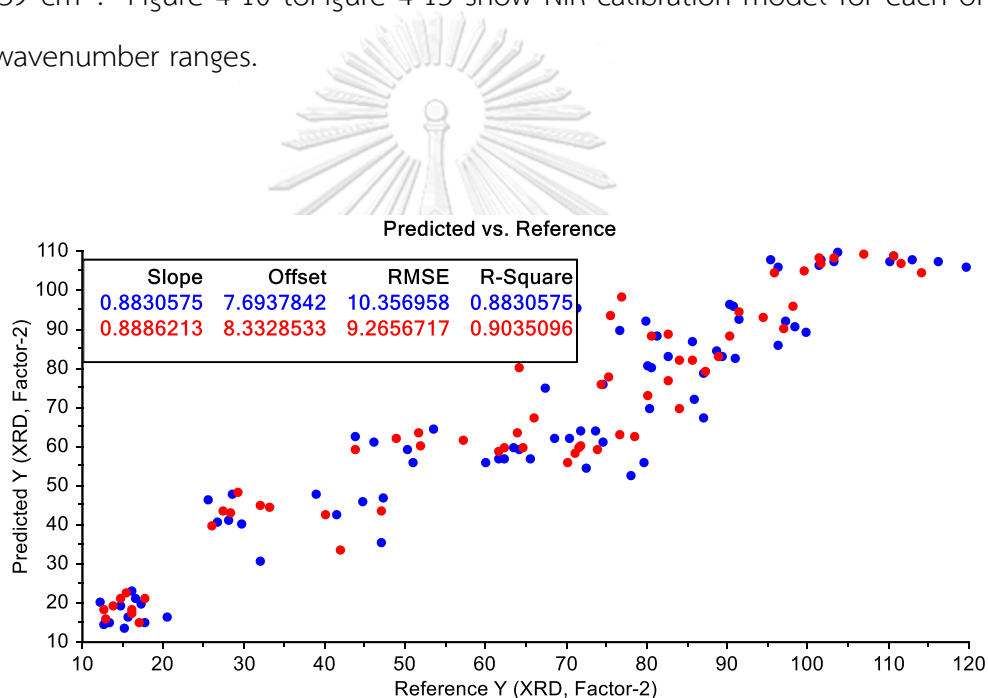


Figure 4-10 NIR calibration model between wavenumber at 4000 – 10000 cm^{-1}

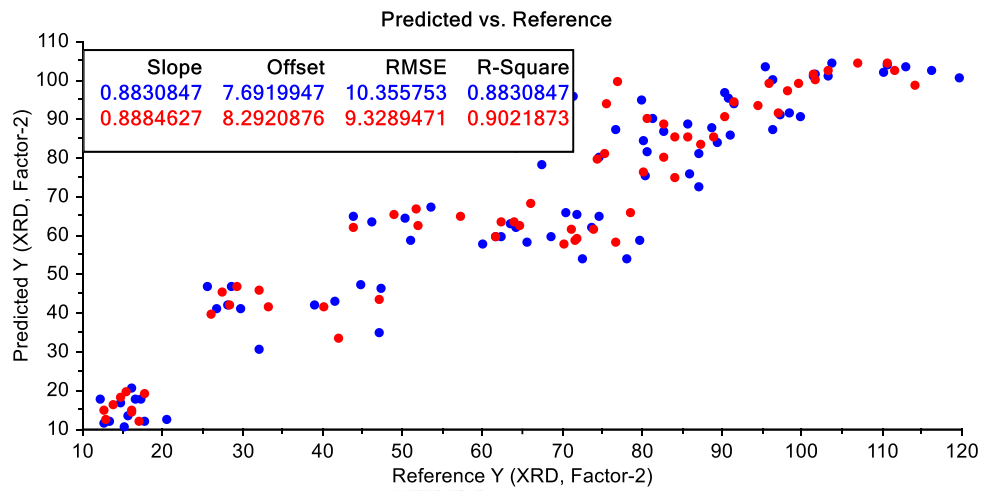


Figure 4-11 NIR calibration model between wavenumber at 4000 – 6000 cm^{-1}

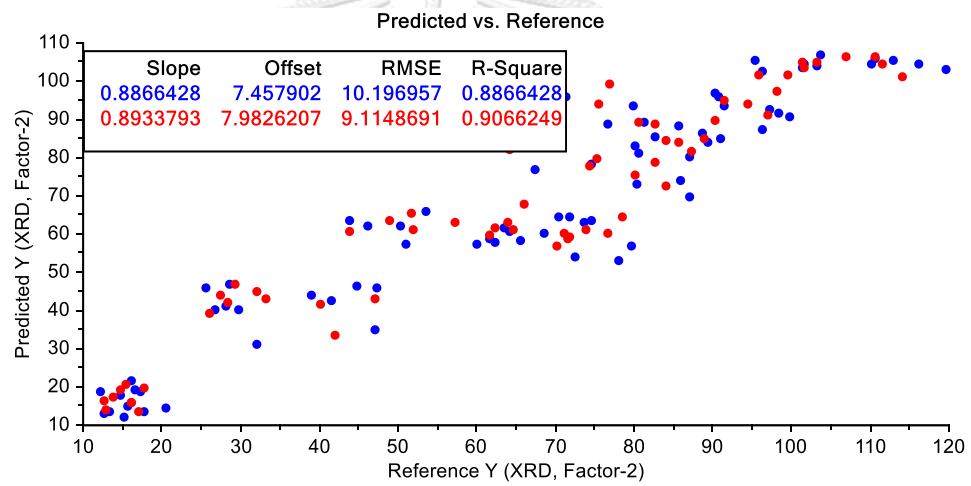


Figure 4-12 NIR calibration model between wavenumber at 4000 – 7600 cm^{-1}

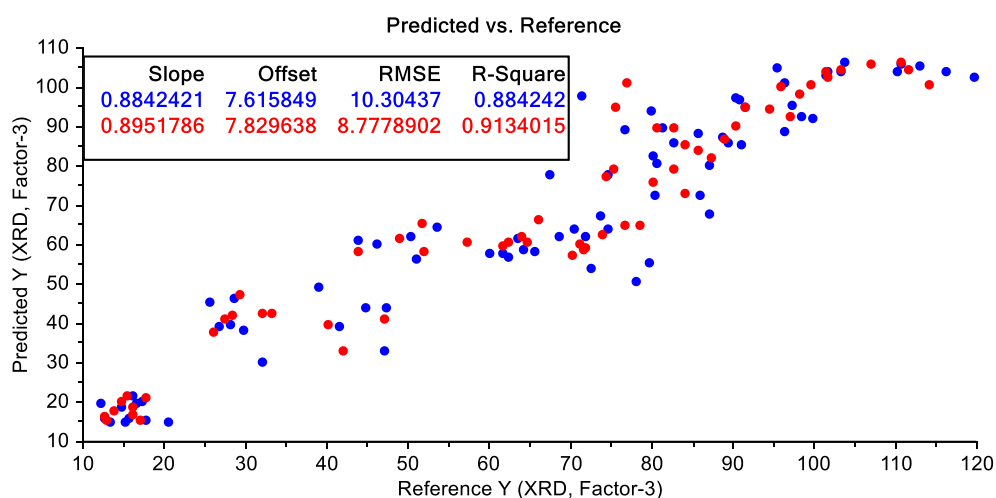


Figure 4-13 NIR calibration model between wavenumber at 6800 – 8700 cm^{-1}

Parameters and results for each calibration range are summarized in Table 4-1. The calibration model assessment was based on RMSEC, RMSEP and the R^2 for each spectral range. The lowest RMSEP and the highest R^2 were determined as suitable model. The results indicated that 6800 - 8700 cm^{-1} range showed the lowest value of RMSEP, thus it was considered as the best range for constructing future calibration model. This result lead to the next step, the pretreatment.

Table 4-1 Spectral range used for developing NIR calibration model

Wavelength (cm^{-1})	RMSEC	R^2	RMSEP	R^2	Factor
4000 - 10000	10.3570	0.8831	9.2657	0.9035	2
4000 - 6000	10.3556	0.8831	9.3289	0.9022	2
4000 - 7600	10.1970	0.8866	9.1149	0.9066	2
6800 - 8700	10.3044	0.8842	8.7779	0.9134	3

Partial least squares (PLS) algorithm results for every calibration model after pretreatment are shown in Table 4-2. Spectral characteristics were different after each pretreatment as shown in Figure 4-14 to Figure 4-17. Values of RMSEC, R^2 of RMSEC, RMSEP and R^2 of RMSEP of non-treated (Figure 4-14) were 10.3044, 0.8842, 8.7779 and 0.9134, respectively. Values of RMSEC, R^2 of RMSEC, RMSEP and R^2 of RMSEP from pretreatment with MSC (Figure 4-15) were 10.2357, 0.8858, 9.1229 and 0.9065,

respectively. Values of RMSEC, R^2 of RMSEC, RMSEP and R^2 of RMSEP from pretreatment with second derivative and Norris-Williams smoothing pretreatment (Figure 4-16) were 10.7066, 0.8750, 9.2305 and 0.9042, respectively. Values of RMSEC, R^2 of RMSEC, RMSEP and R^2 of RMSEP from pretreatment with MSC, second derivative and Norris-Williams smoothing (Figure 4-17) were 9.9486, 0.8921, 8.2495 and 0.9235, respectively.

The spectral pretreatment using MSC followed by second derivative and Norris-Williams (No. 10) showed the lowest value of RMSEP and highest R^2 value. Therefore, it was chosen as the calibration model for real-time process monitoring.

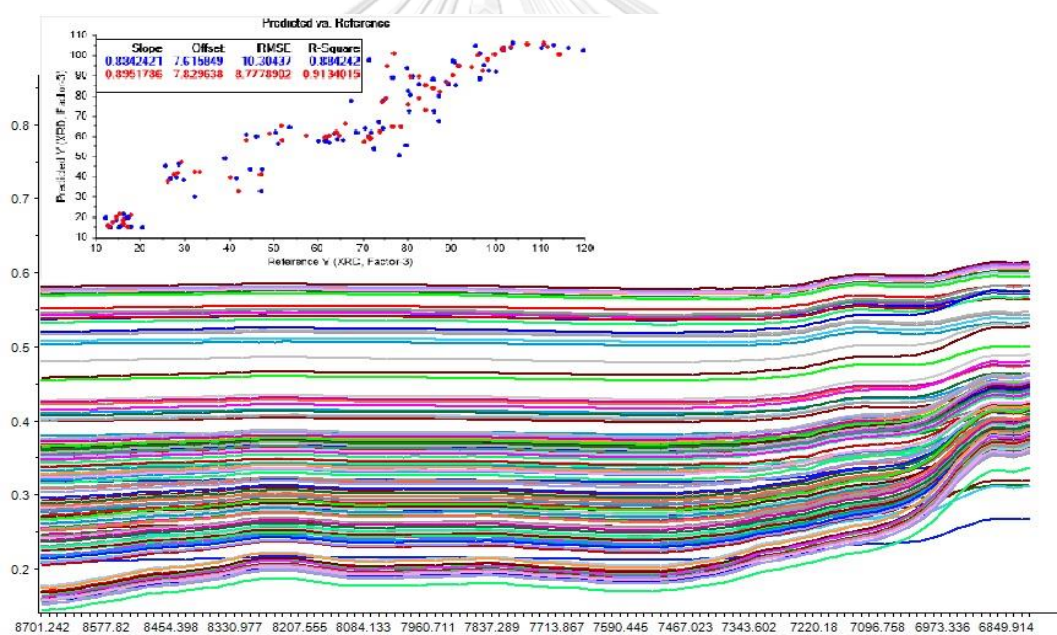


Figure 4-14 Calibration model (in-set) and non-treated of NIR spectra

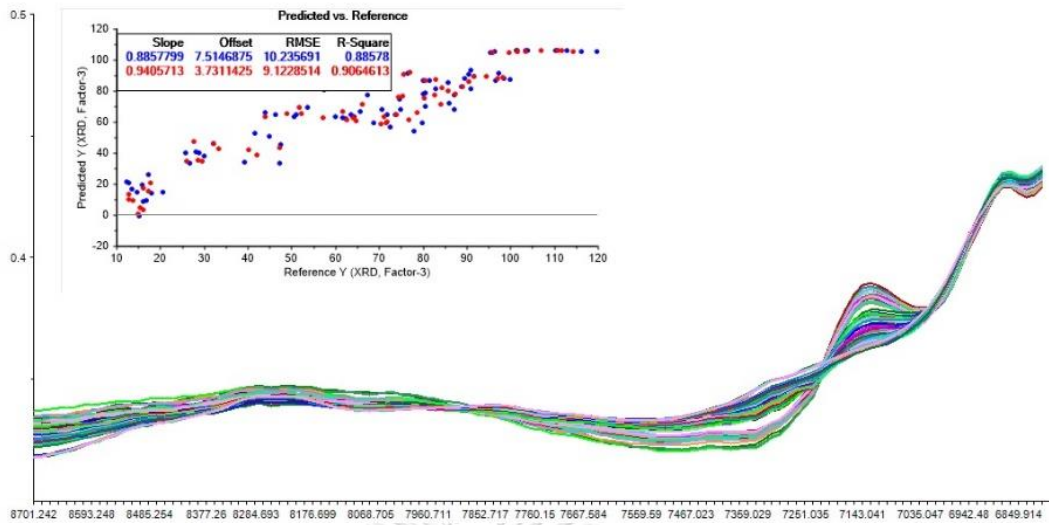


Figure 4-15 Calibration model (in-set) of NIR spectra after MSC pretreatment

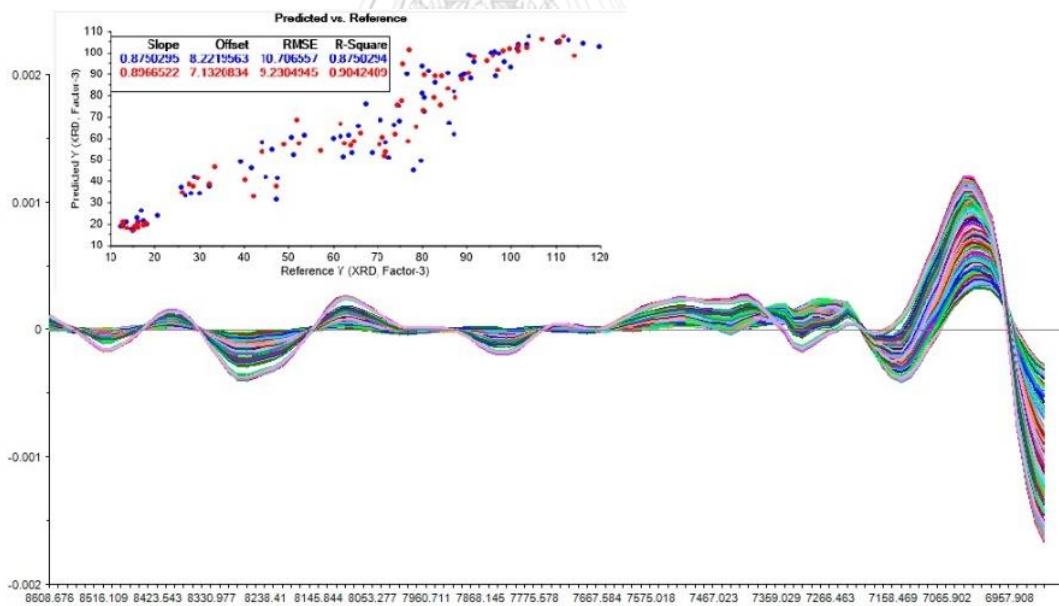


Figure 4-16 Calibration model (in-set) of NIR spectra after
2nd derivative + Norris-Williams pretreatment

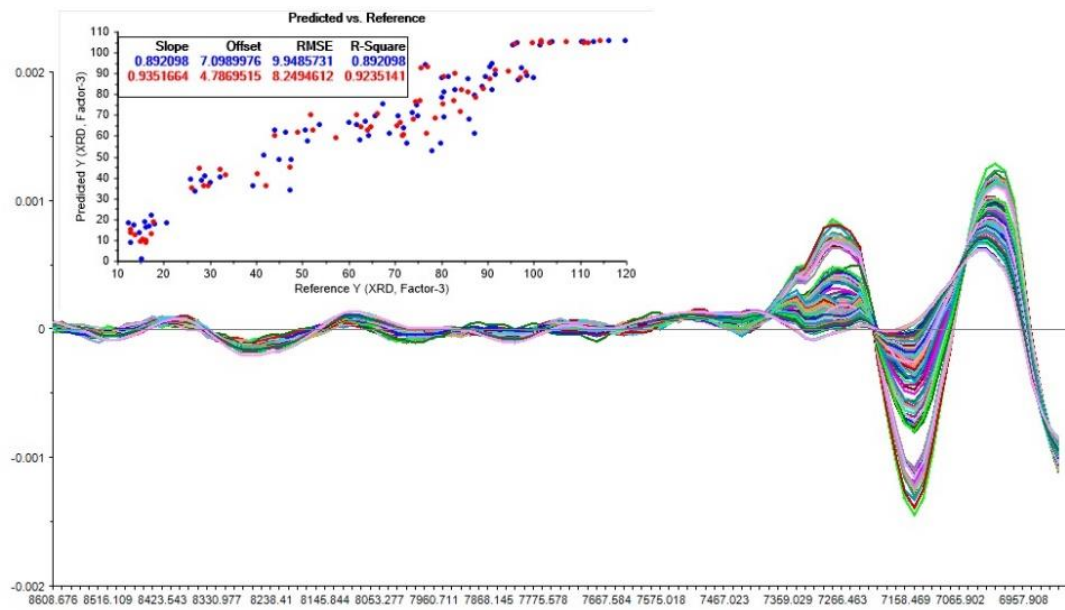


Figure 4-17 Calibration model (in-set) of NIR spectra after
MSC + 2nd derivative + Norris-Williams pretreatment

Table 4-2 Pretreatment of NIR calibration model in the region of 6800 - 8700 cm^{-1}

No.	First step	Second step		RMSEC	R ²	RMSEP	R ²	Factor
		Derivative	Smoothing					
1	-	-	-	10.3044	0.8842	8.7779	0.9134	3
2	-	1 st	Norris-Williams	10.4722	0.8804	9.7444	0.8933	3
3	-	1 st	Savitzky-Golay	10.4686	0.8805	9.7320	0.8936	3
4	-	2 nd	Norris-Williams	10.7066	0.8750	9.2305	0.9042	3
5	-	2 nd	Savitzky-Golay	10.6464	0.8764	9.1416	0.9061	3
6	MSC	-	-	10.2357	0.8858	9.1229	0.9065	3
7	SNV	-	-	10.1329	0.8881	9.0424	0.9081	3
8	MSC	1 st	Norris-Williams	9.9659	0.8917	8.5099	0.9186	3
9	MSC	1 st	Savitzky-Golay	9.9733	0.8916	8.4834	0.9191	3
10	MSC	2 nd	Norris-Williams	9.9486	0.8921	8.2495	0.9235	3
11	MSC	2 nd	Savitzky-Golay	10.0092	0.8908	8.2982	0.9226	3
12	SNV	1 st	Norris-Williams	9.9048	0.8930	8.4060	0.9206	3
13	SNV	1 st	Savitzky-Golay	9.9116	0.8929	8.3967	0.9208	3
14	SNV	2 nd	Norris-Williams	9.9358	0.8926	8.3453	0.9217	3
15	SNV	2 nd	Savitzky-Golay	9.9579	0.8919	8.3567	0.9215	3

3. Real-time continuous mixing process monitoring

The mixing process was done by using in-house vertical mixer as shown in Figure 3-1 and Figure 4-18. This experiment aimed to determine the steady-state of mixing while using vertical continuous mixer. The definition of steady-state phase in this experiment is the almost constant movement of concentrations during a specified time range, which can be either equal to or unequal to the expected target concentration.

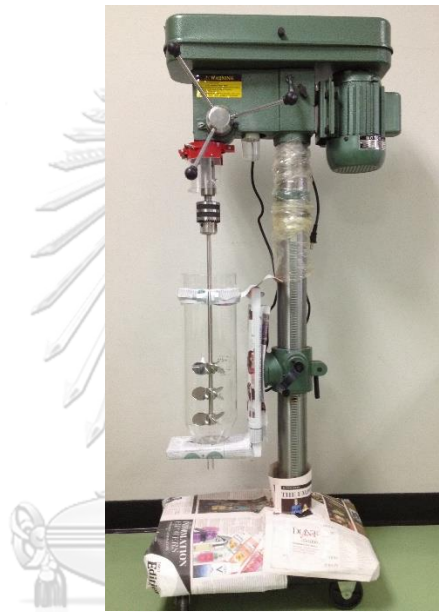


Figure 4-18 In-house vertical mixer for continuous mixing process

The mixing uniformity of continuous mixing process was initially measured by calculating percent relative standard deviation (%RSD) on NIR spectra. Moving block average of ten consecutive concentrations were taken continuously while mixing and were calculated for %RSD from the beginning of the process to the end. Normally, when %RSD was lower than 5% for ten consecutive moving measurements, the mixture was assumed to reach homogeneity(39).

Percent relative standard deviation (%RSD) of NIR probe position no.1 (trial A, C, E and G) were a continuously smooth line while NIR probe position no.2 (trial B, D, F and H) showed more irrational patterns due to in higher mixing turbulence

of powder between impellers no.2 and no.3. Concentration of spray dried lactose was decreased when iron powder was first introduced into the chamber with spray dried lactose in early numbers of RSD blocks. Resulting in unstable %RSD values which tend to increase in the initial phase of mixing. After the process reached steady-state, %RSD decreased due to concentrations moving in a narrow range. However, some concentrations during steady-state were higher than others causing the higher %RSD in some blocks. During depletion phase, %RSD are drastically higher at the end of RSD blocks because materials depleted.

Values of %RSD obtained in this experiment were below 5% threshold since the beginning of the process. These results show that the differences in %RSD values were insufficient to determine steady-state of mixing. Percent RSD was not able to detect the minor differences in the concentrations throughout the mixing process. This is possibly due to the uniformity of the concentration data collected. As a result, %RSD was not used for steady-state determination. When %RSD was not appropriate to be used to differentiate between phases during mixing, basic scattered concentration plots were used instead. Predicted NIR concentrations compared to %RSD in each trial are shown in Figures 4-19 to 4-34.

Similar average concentrations are found between trial A (85.47 ± 1.53 %w/w) and B (85.90 ± 1.89 %w/w) in steady-state phase. This indicated that the concentrations determined by NIR probe positions, no.1 and 2, of the aligned impellers with 0.5-inch distance, homogeneous from top to bottom during steady-state.

Trial C (85.76 ± 1.46 %w/w) and D (84.27 ± 1.51 %w/w) showed the lowest value of the average NIR concentrations in steady-state among all trials. Especially, trial D showed the closest value to the set target concentration of 80 %w/w. These indicated that NIR position no. 2 of the opposite impeller alignment with 0.5-inch distance shows the best mixing performance.

Trial E (90.56 ± 1.39 %w/w) showed higher value of the average NIR concentrations in steady-state phase than trial F (89.40 ± 2.08 %w/w). The results

indicated that NIR position no. 2 of the aligned impeller with 1.0-inch distance shows better mixing property than no.1. Gradual mixing homogeneity was achieved and seen from top to bottom.

Trial G (89.43 ± 1.84 %w/w) showed higher value of the average NIR concentrations in steady-state phase than trial H (87.91 ± 1.97 %w/w). The result indicates that NIR position no. 2 of the aligned impeller with 1.0-inch distance shows better mixing property than no.1, which is similar to the comparison results between trial E-F and C-D.



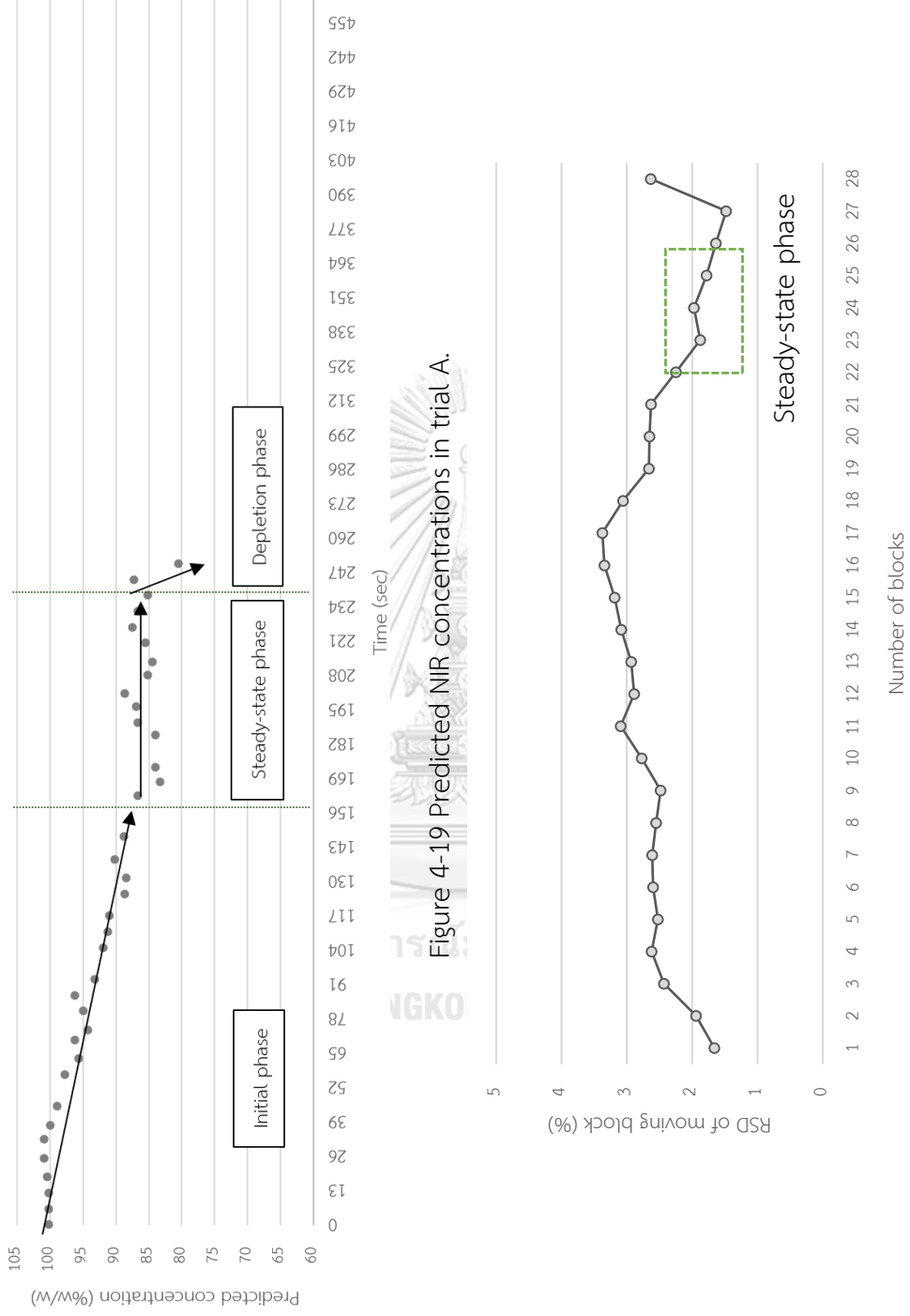


Figure 4-19 Predicted NIR concentrations in trial A.

Figure 4-20 %RSD of moving block concentrations average from trial A.

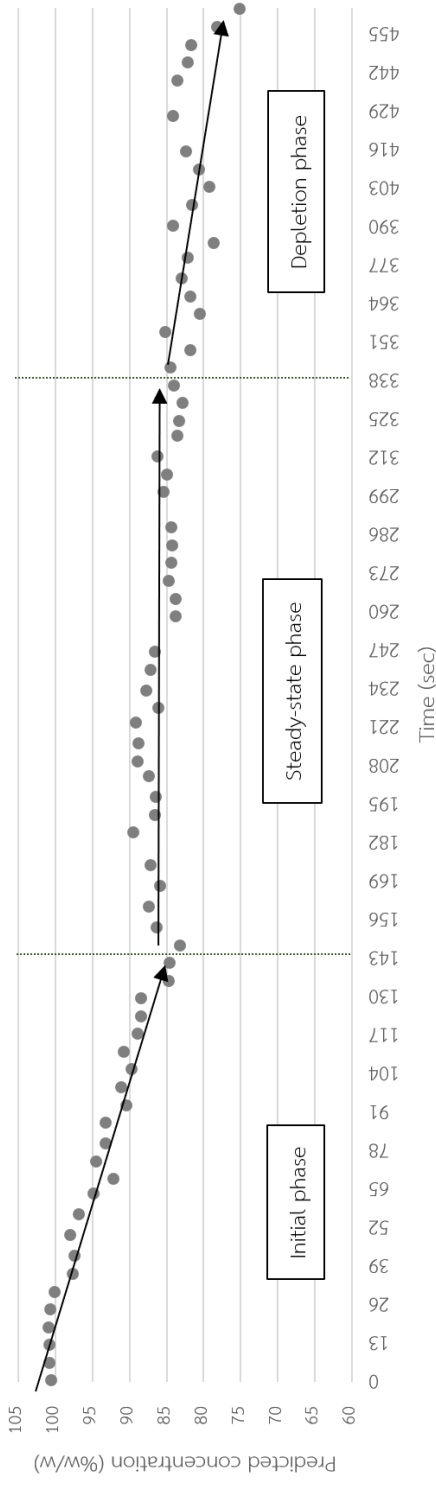


Figure 4-21 Predicted NIR concentrations in trial B.

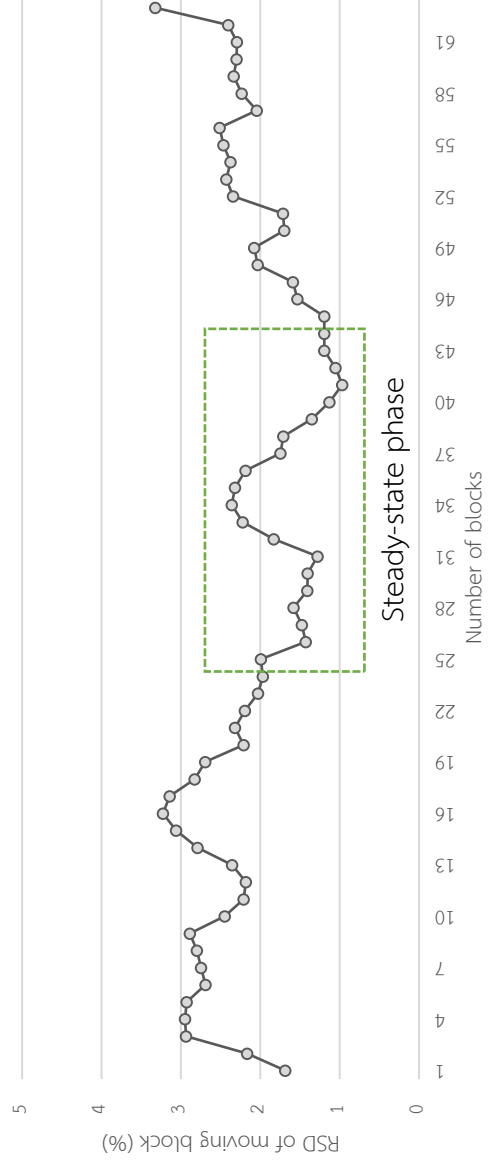


Figure 4-22 %RSD of moving block concentrations average from trial B.

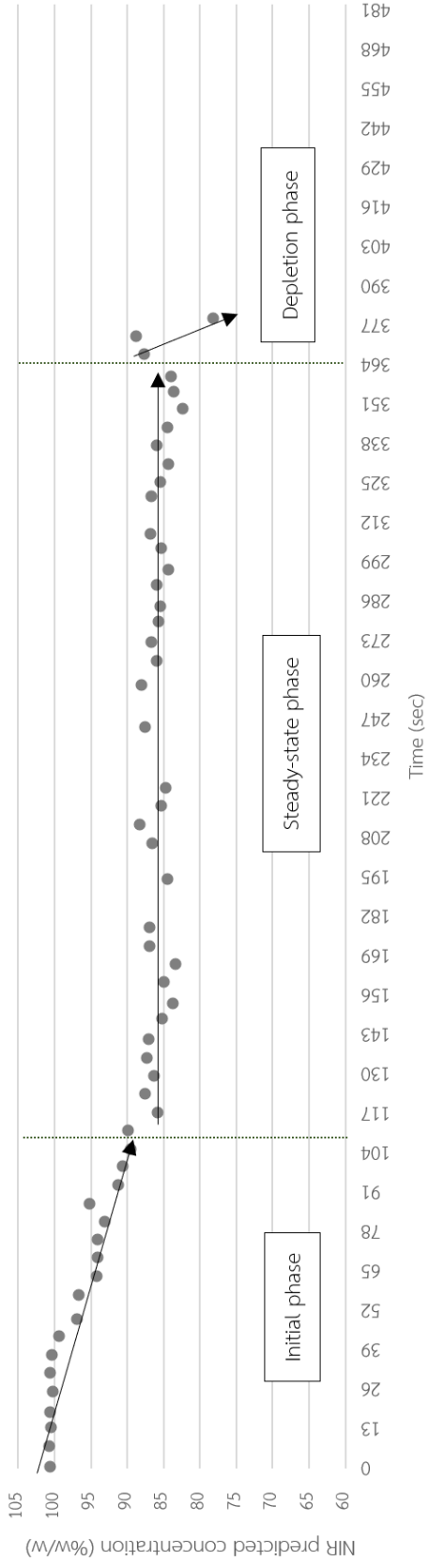


Figure 4-23 Predicted NIR concentrations in trial C.

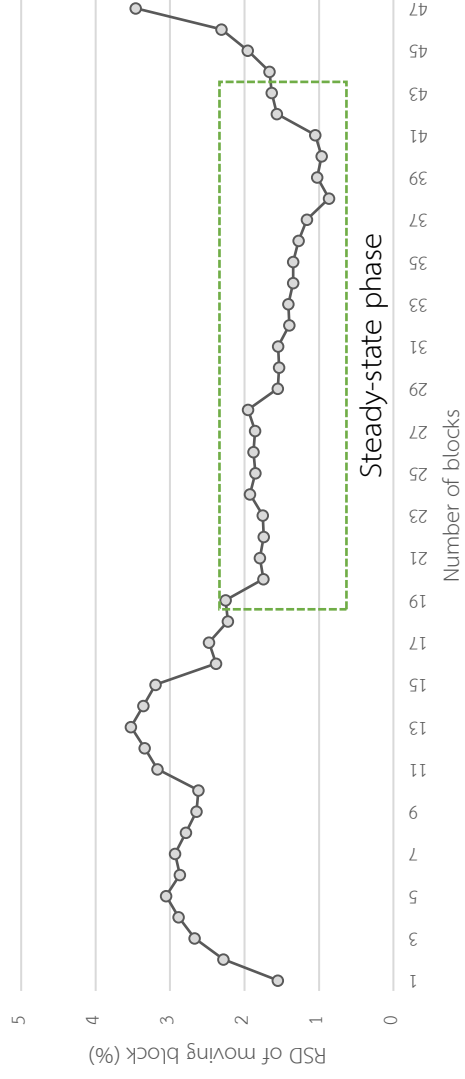


Figure 4-24 %RSD of moving block concentrations average from trial C.

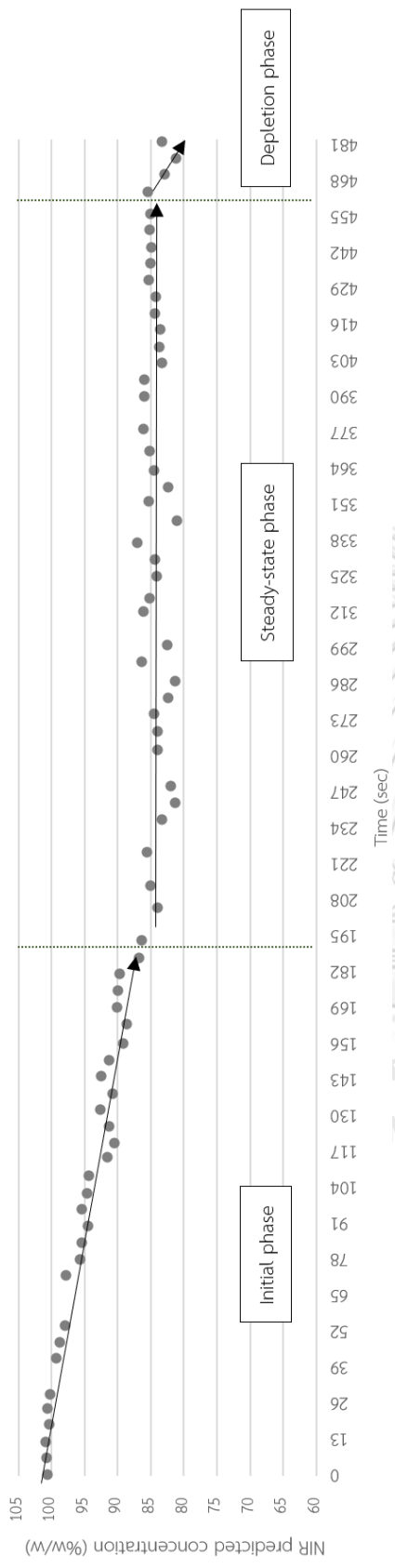


Figure 4-25 Predicted NIR concentrations in trial D.

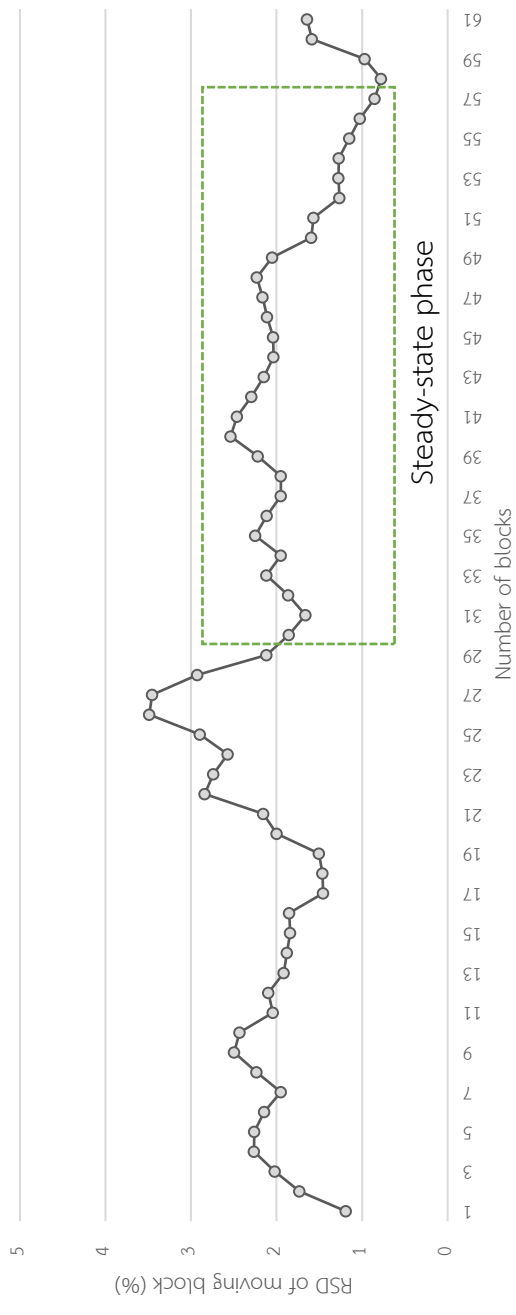


Figure 4-26 %RSD of moving block concentrations average from trial D.

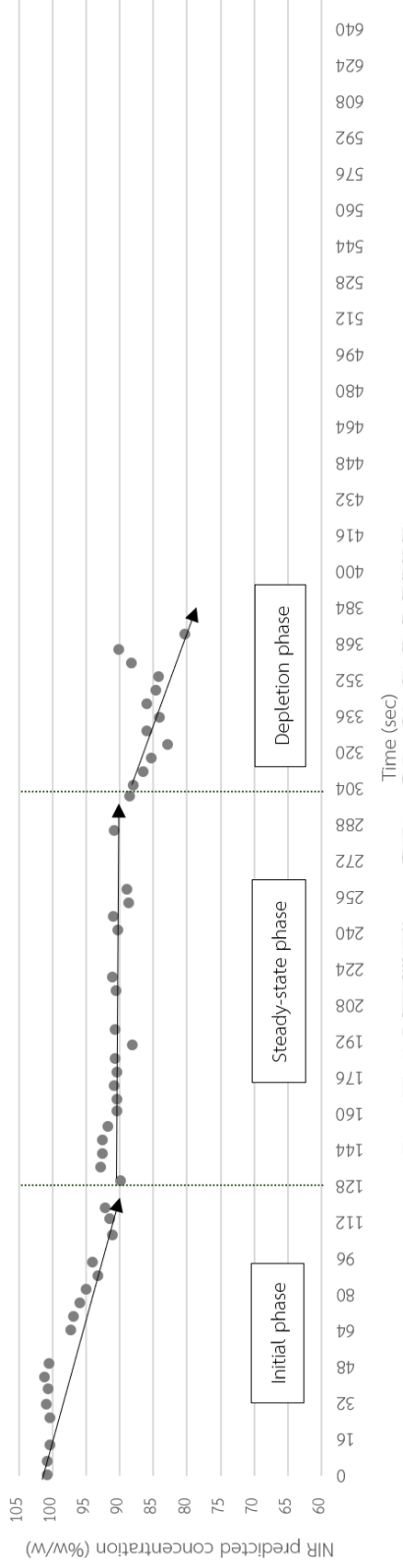


Figure 4-27 Predicted NIR concentrations in trial E.

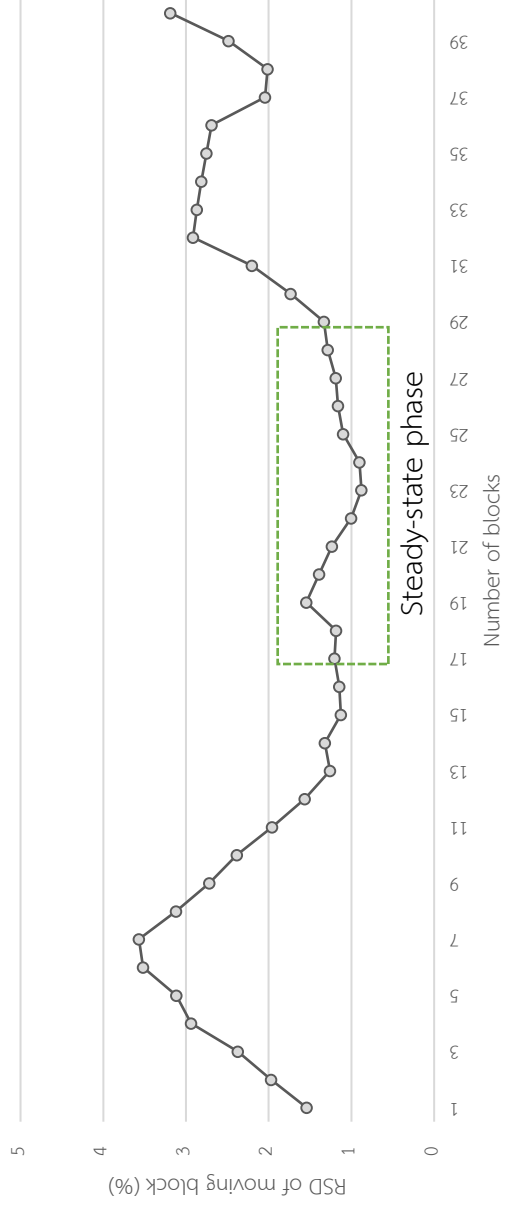


Figure 4-28 %RSD of moving block concentrations average from trial E.

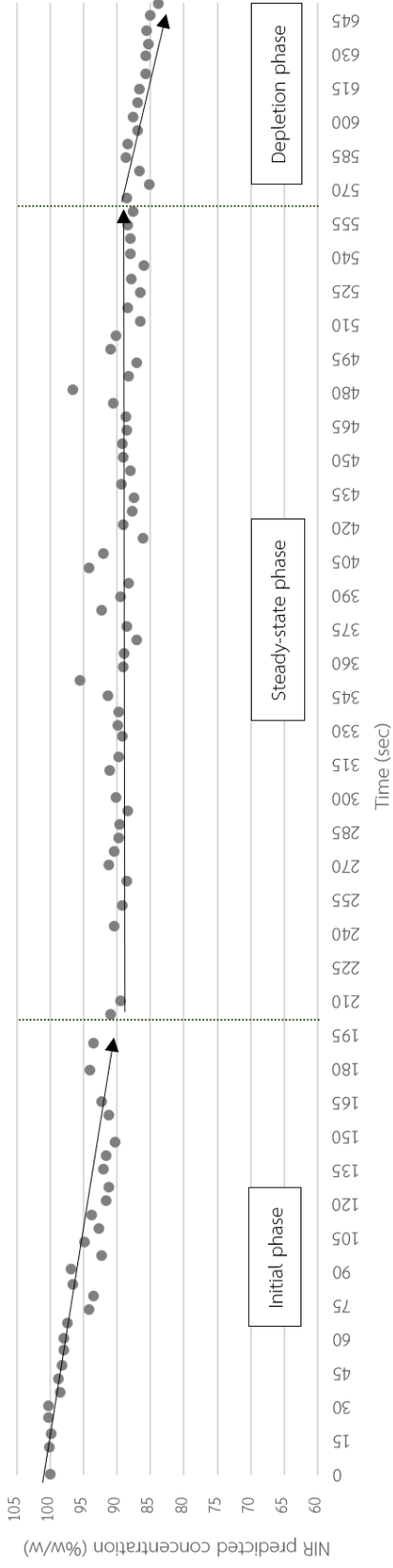


Figure 4-29 Predicted NIR concentrations in trial F.

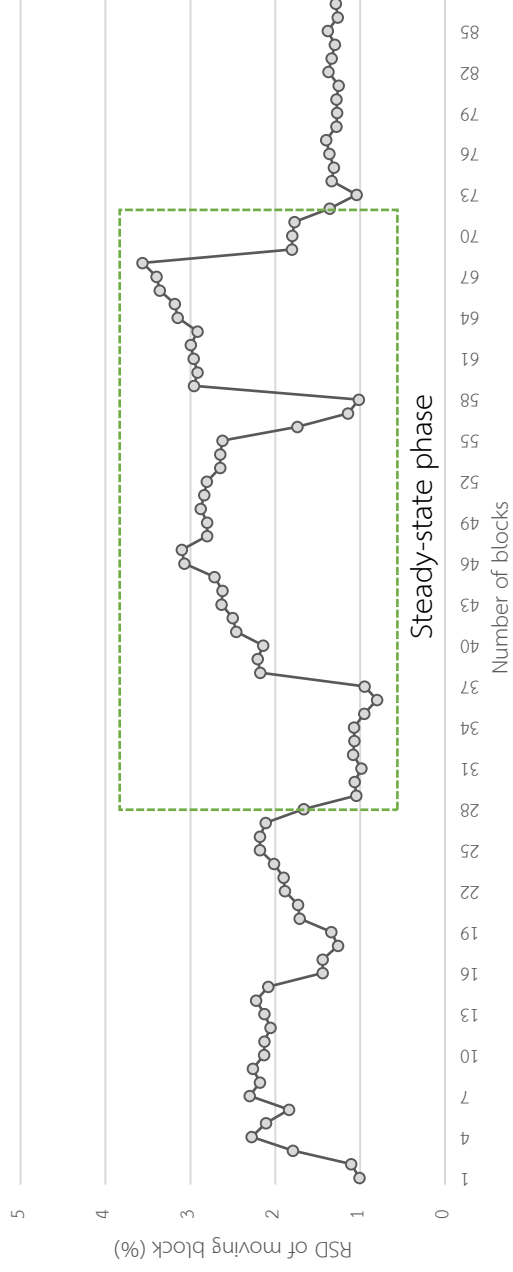


Figure 4-30 %RSD of moving block concentrations average from trial F.

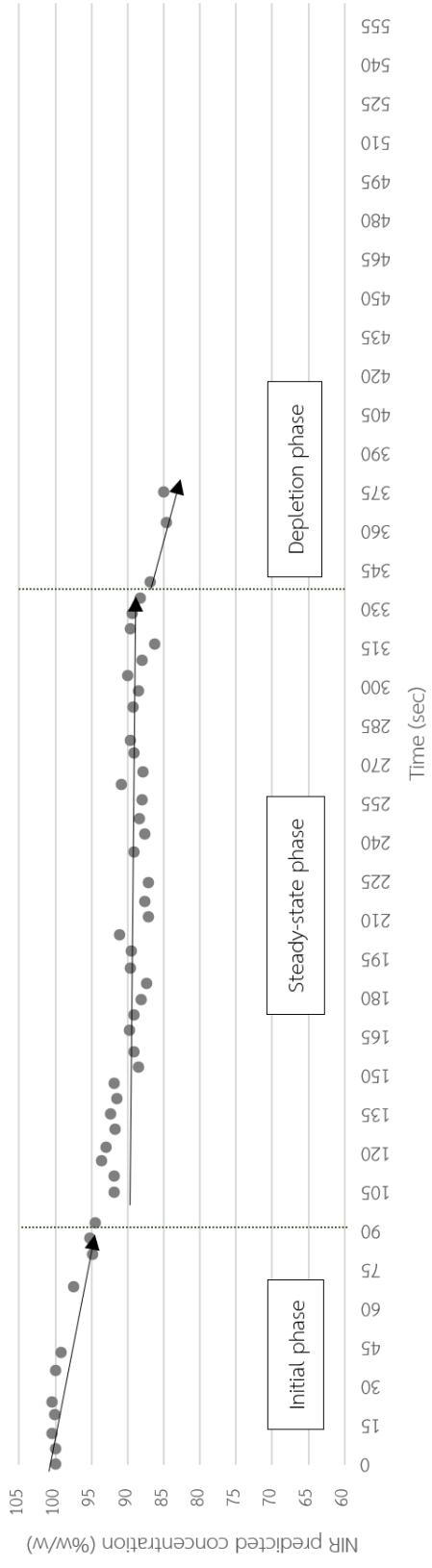


Figure 4-31 Predicted NIR concentrations in trial G.

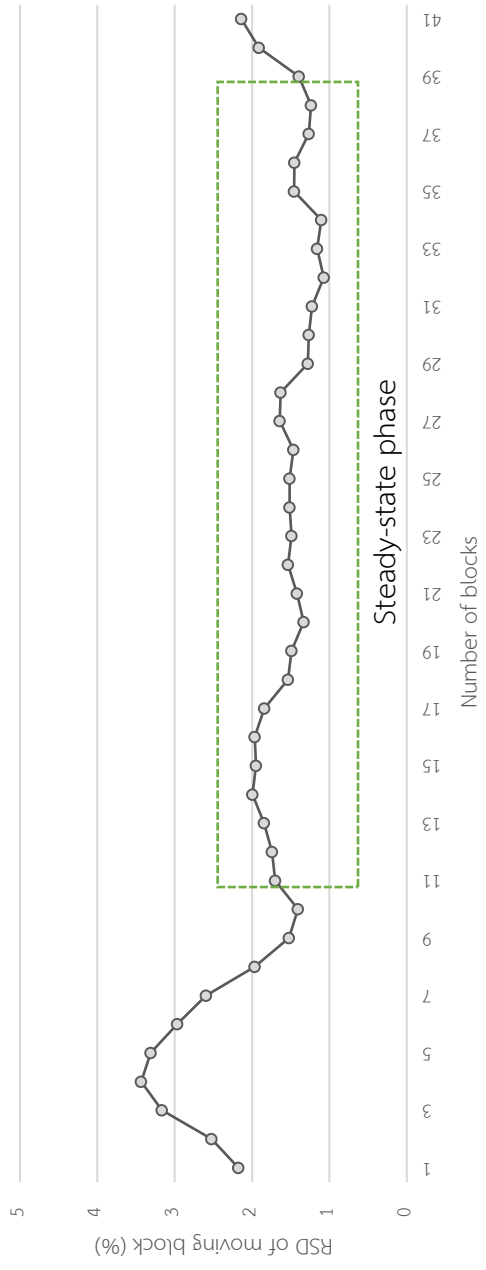


Figure 4-32 %RSD of moving block concentrations average from trial G.

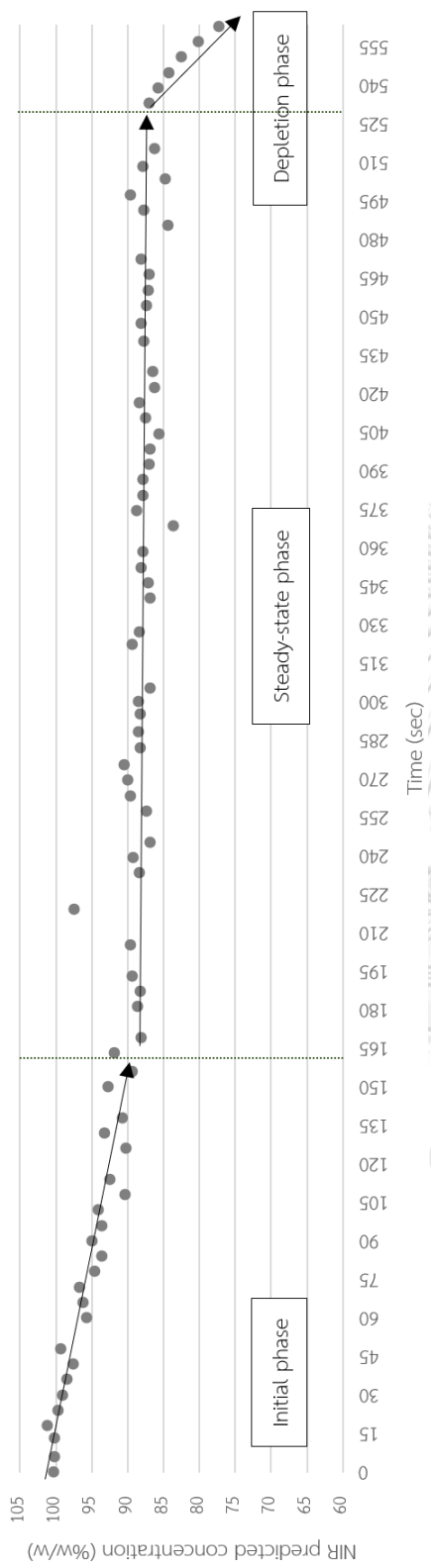


Figure 4-33 Predicted NIR concentrations in trial H.

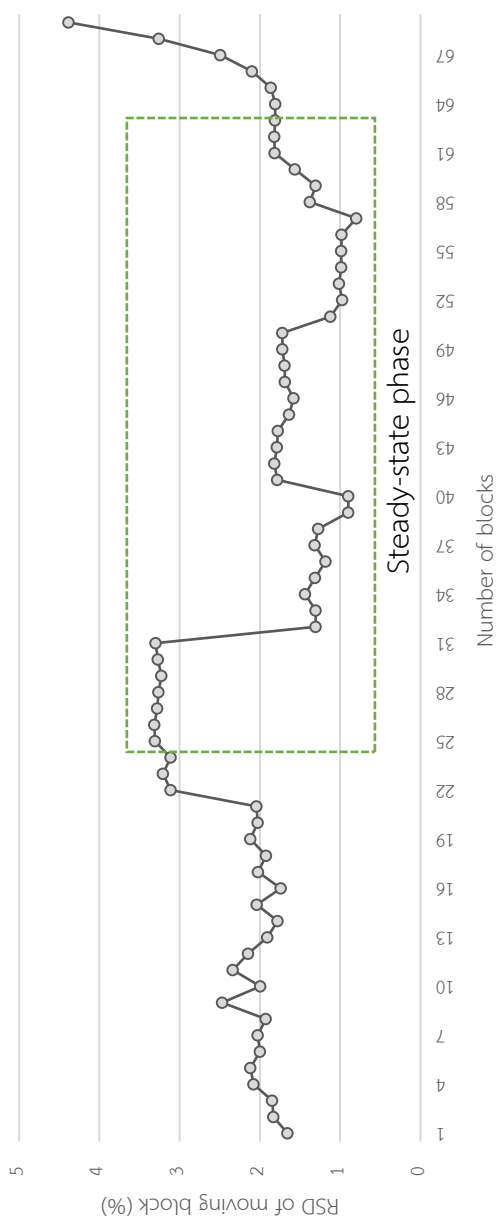


Figure 4-34 %RSD of moving block concentrations average from trial H.

Concentration results for continuous mixing process could be divided into three phases: initial, steady-state and depletion as seen in Figure 4-35. Initial phase was the period that the concentration of spray dried lactose in the mixture was reduced. The mixing chamber was initially filled with spray dried lactose before iron powder was added through the hopper. Consequently, the concentration of the mixture was decreased by iron powder. The concentration continually decreased until it was stable, hence, the steady-state phase was reached. This phase shows the movement of concentrations are in a very narrow range so that the process reaches equilibrium between inflow and outflow mass. The process continued in this phase until the materials in the hoppers are depleted. In the depletion phase, the amount of the remaining mixture in the chamber was gradually decreased due to no powder input. The detection process ended when the last powder mixture moved pass lower (no.2) NIR probe.

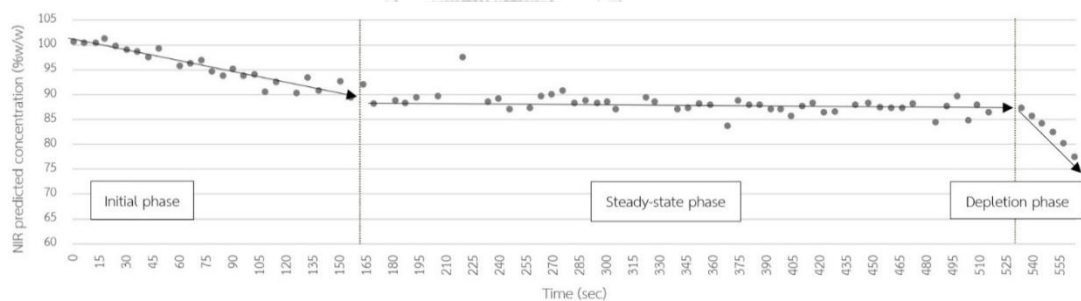


Figure 4-35 Concentrations of three phases of trial H during continuous mixing process obtained by NIR: Initial, steady state and depletion.

3.1. Onset time of steady-state

Onset time of steady-state phase from trial A to H started after the mixing process began within 162, 147, 111, 193, 130, 204, 93 and 163 seconds, respectively (Figure 4-36). Steady-state onset should be monitored from the beginning of the mixing process at NIR probe position no.1. When compare between impeller alignments (opposite and aligned) in both impeller distances (0.5 and 1.0-inch), results show that steady-state onset of opposite impeller alignments, trial C (0.5-inch impeller distance) and trial G (1.0-inch impeller distance), were faster than aligned impellers, trial A (0.5-inch impeller distance) and trial E (1.0-inch impeller distance).

For continuous manufacturing, all materials are continuously loaded into the mixer. Steady-state obtained in continuous mixing process will remain unchanged if materials are still continuously fed into the mixing chamber. Hence, the most important factor is the total quantity of materials used in each trial which will determine the steady-state duration. Thus, duration of steady-state is not associated with design parameters of the mixer such as the impeller alignment and distance between impellers.

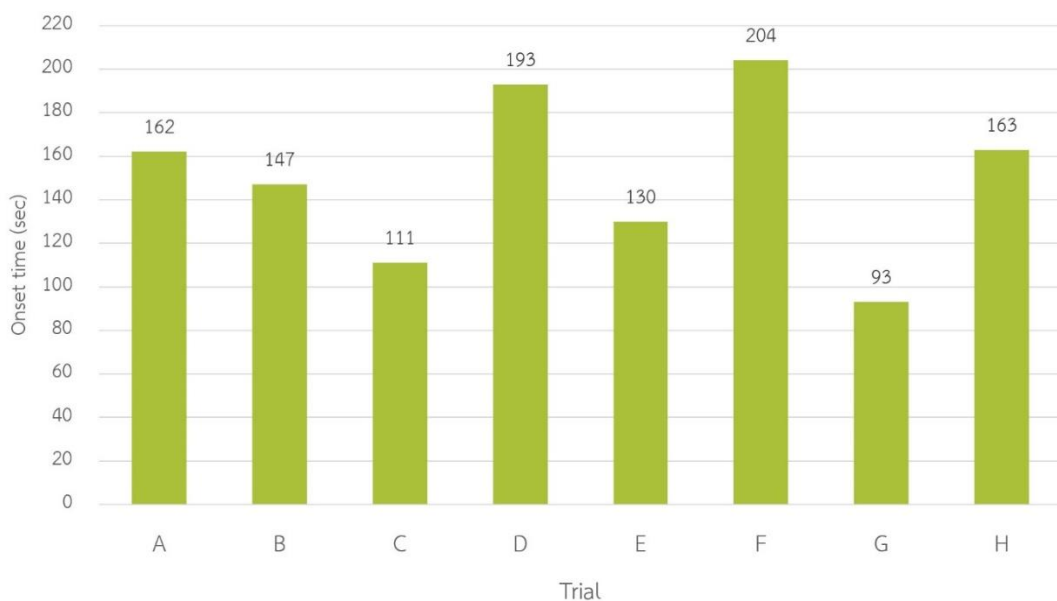
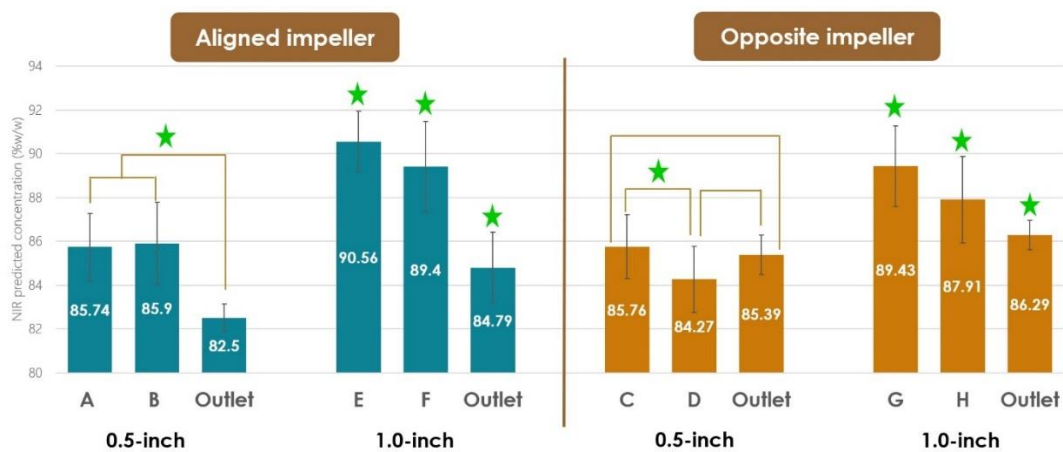


Figure 4-36 Steady-state reached in each trial.

3.2. Mixing performance

The average concentration in each trial (A to H) and average concentration of final mixture at the outlet for each impeller alignment with different impeller distance during steady-state was compared by calculating 95% confidence interval and the results are shown in Figure 4-37.



★ significantly different ($p < 0.05$)

Figure 4-37 Statistical comparisons of average mixture concentrations from trial A to H and concentration final mixtures collected at the outlet during steady-state.

The similarity of concentrations for top and bottom positions for both impeller alignments at 0.5-inch distance (Figure 4-37) represents good mixing performance which shows the robustness of measurements regardless of positions where NIR measurements were taken.

For aligned impeller with 0.5-inch distance, there was no significant difference between trial A and B which were the concentration in real-time measurement at NIR probe positions no.1 and no.2, respectively. However, both trial A and B were different from the final mixture at the outlet where the concentration of mixture was decreased when the mixture moved from NIR probe position no.1 to the outlet. For opposite impeller with 0.5-inch distance, there was no significant difference between final mixture at the outlet. However, concentration at NIR probe position no.1 was slightly

different from concentration at NIR probe position no.2 while concentration of mixtures increased when approaching the outlet. These results indicated that 0.5-inch impeller distance shows a good mixing performance for both impeller alignments.

On the other hand, concentration of mixtures in 1.0-inch impeller distance for both aligned impeller and opposite impeller show significant difference in every NIR probe positions and outlet. Concentration of mixtures were significantly decreased from the NIR probe positions no.1 to no.2 and to the outlet. It would seem that 1.0-inch impeller distance was affected by different NIR probe positions. Thus, 1.0-inch impeller distance for both impeller alignments show less robustness in measurement positions.

3.3. Target concentration reached in real-time measurement

From Figure 4-38, concentrations obtained by NIR of aligned impellers with 0.5-inch distance in trial A and B were lower and were closer to the set target than 1.0-inch distance in trial E and F. Furthermore, opposite impeller alignments showed similar results as the aligned impeller. Concentration of trial C and D (0.5-inch distance) were lower and were closer to the set target than trial G and H (1.0-inch distance). These results indicated that the predicted NIR concentrations and blend uniformity of mixtures are affected by the distance between impellers. As a result, 0.5-inch impeller distance led to homogeneity of mixtures for both impeller alignments.

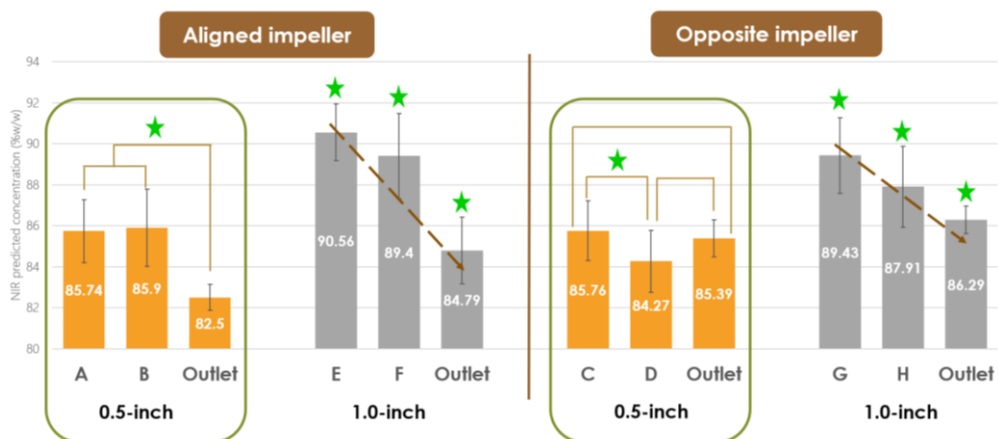


Figure 4-38 Mixture concentrations during steady-state.

3.4. Accuracy of final target concentration mixtures

Mixtures which were collected from the outlet while in steady-state phase were analyzed with off-line NIR for their concentrations. The results show that average predicted NIR concentration of the aligned impeller with 0.5-inch impeller distance resulted in the closest values to the set target concentration, follow by aligned impeller with 1.0-inch distance, and finally opposite impeller alignment with 0.5-inch and 1.0-inch distance, respectively.

The average predicted sample concentrations obtained by NIR for impellers set-up with 0.5-inch distance was closer to the target concentration than 1.0-inch set-up for both impeller alignments as shown in Figure 4-39. These results suggest that set-up of impellers with 0.5-inch distance could lead to accuracy and homogeneity of the final mixture better than when impellers are kept apart at 1.0-inch. It seems that the distance between impellers is one of the process parameters which affect the target concentration and homogeneity of the final mixture.

When considering the alignment of impellers in mixtures collected from outlet, impellers with the aligned direction was closer to the target concentration than opposite impeller alignments for both impeller distances as shown in Figure 4-39. This result suggests that the alignment of impeller affect mixing dynamics and blend uniformity. The aligned impellers led to better homogeneity of the final mixture due to the movement of powder in a consistent uniform flow direction from top to bottom. However, the powder which are mixed with opposite impeller alignments may move upward when they meet with another direction of lower impellers. This situation caused turbulence of the powder which effect non-uniform flow of the mixture. The iron powder remained on the upper portion of the chamber, so the NIR concentration of spray dried lactose was higher than it expected. After steady-state, a decreasing concentration to the lowest average concentration occurred. This result may be due

to the increasing amount of iron powder in the mixture moving from the upper to lower portion of the chamber, while spray dried lactose were depleted.

Hence, process parameters which affected accuracy of final target concentration are the distance between impellers (0.5-inch > 1.0-inch) and the alignment of impeller set-up (aligned > un-aligned).

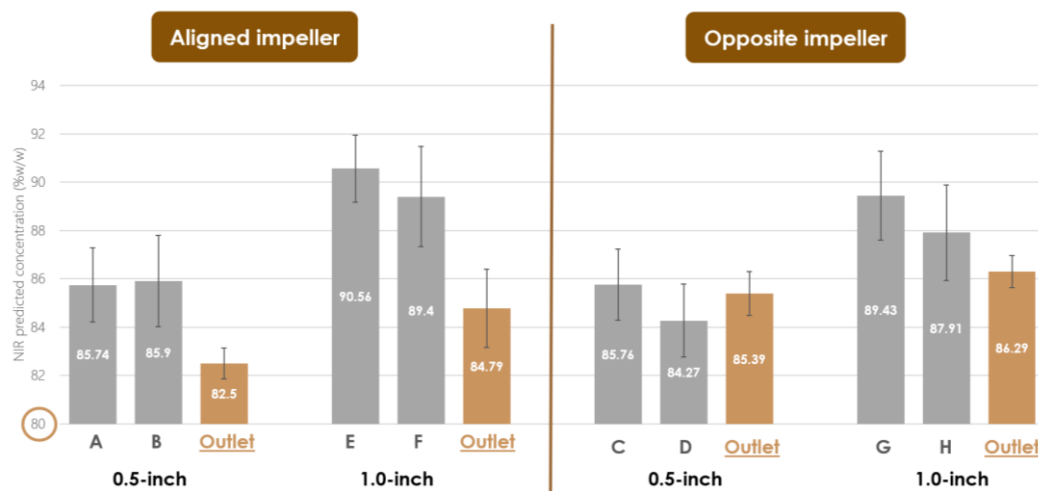


Figure 4-39 Final mixture concentrations collected from outlet during steady-state.

CHAPTER V

CONCLUSION

In this study, near-infrared spectroscopy was used for real-time monitoring of the mixing phases in the continuous powder mixing process. A vertical continuous mixer built in-house was used for mixing model substances, spray dried lactose and iron powder. Spectra, obtained from NIRs, were pretreated and were developed to an appropriate calibration model by using partial least squares (PLS) algorithm. The influence of mixer design parameters on the concentration of mixture in the steady-state was investigated by varying impeller alignment and the distance between impellers.

Spectral wavenumber of $6800 - 8700 \text{ cm}^{-1}$ was selected for calibration model development. Pretreatment with MSC, second derivative and Norris-Williams smoothing showed the lowest RMSEP, hence, it was chosen for development of the calibration equation with PLS for real time process monitoring.

During steady-state phase, the average predicted NIR concentrations were calculated %RSD in each moving block of ten consecutive concentrations for evaluating the homogeneity of the mixtures and were statistically compared by one-way ANOVA with 95% confidence interval.

The difference in %RSD patterns were affected by the position NIR probe was placed. NIR probe position no.1 shows smooth %RSD patterns. NIR probe position no.2, however, shows more irrational patterns. Initially, %RSD increased in the early phase of mixing, decreasing when in steady-state and sharply increased during depletion phase.

Results from every trial show that %RSD could not be used to detect different mixing phases during continuous mixing due to the similarity of the data. Consequently, basic concentrations were plotted against time to identify different phases during continuous mixing.

Three phases were identified from predicted NIR concentrations which composed of initial, steady-state and depletion. Both, the alignment of impellers and distance between impellers were found to effect blend uniformity of the mixture. Opposite impeller alignments reached steady-state faster than aligned impeller in both impeller distances (0.5 and 1.0-inch). Mixing performance was evaluated from the similarity of concentrations in every measurements. The results show that 0.5-inch impeller distance shows a good mixing performance for both impeller alignments (aligned and opposite). Impeller distance of 0.5-inch was found to result in the concentration closer to target concentration than 1.0-inch distance for both impeller alignments leading to homogeneity of mixtures. Set-up of impellers with 0.5-inch distance could lead to homogeneity of the final mixture better than when impellers were kept apart at 1.0-inch distance. The homogeneity of the final mixture reaching target concentration could be obtained via the aligned directional alignment rather than the opposite impeller alignment due to the movement of powder in a uniform flow direction.

Better mixing could be achieved with 0.5-inch impeller distance due to higher mixing force of closer impeller distances. However, further impeller distances (1.0-inch impeller distance) shows concentration differences for both probe positions because of independently movement of mixtures.

Aligned impeller led to higher homogeneity because mixtures were freely flowing from top to bottom in the same direction with no turbulence flow. However, opposite impeller alignment caused turbulence flow of powder traveling from top to bottom by contacting the 90° blade positioned below.

The results of continuous mixing process monitor during steady-state can be divided into 4 parts as shown in Figure 5-1. Aligned impellers with 0.5-inch distance (Figure 5-2) is found to be the best mixing set-up which leads to the homogeneity of the mixtures as can be seen by the best mixing performance, measurement robustness

and accuracy in achieving final target concentration. However, the limitation of this set-up is that this condition has longer onset time for steady-state.

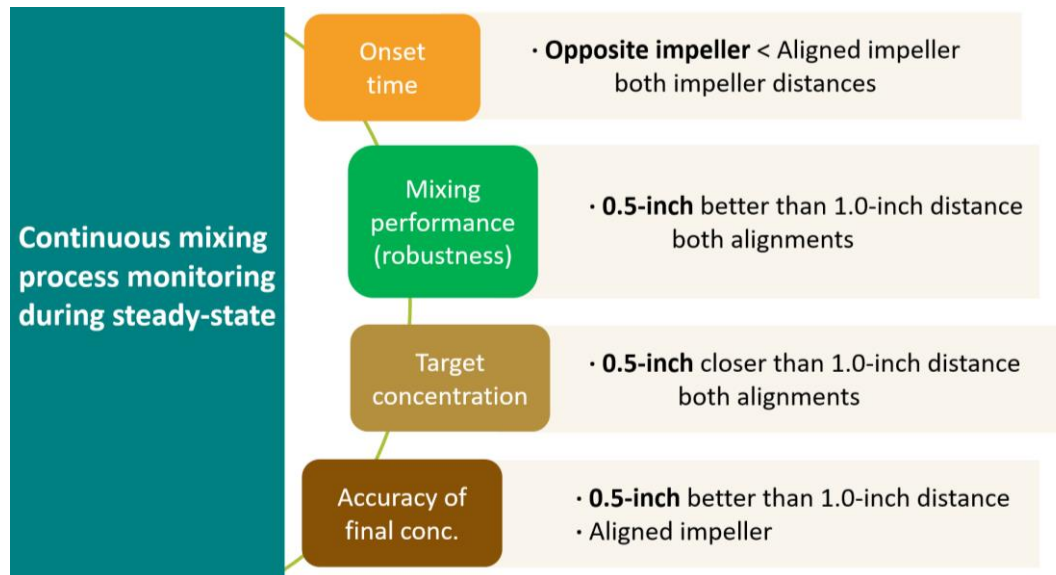


Figure 5-1 Result summary on factors affecting continuous mixing process during steady-state.

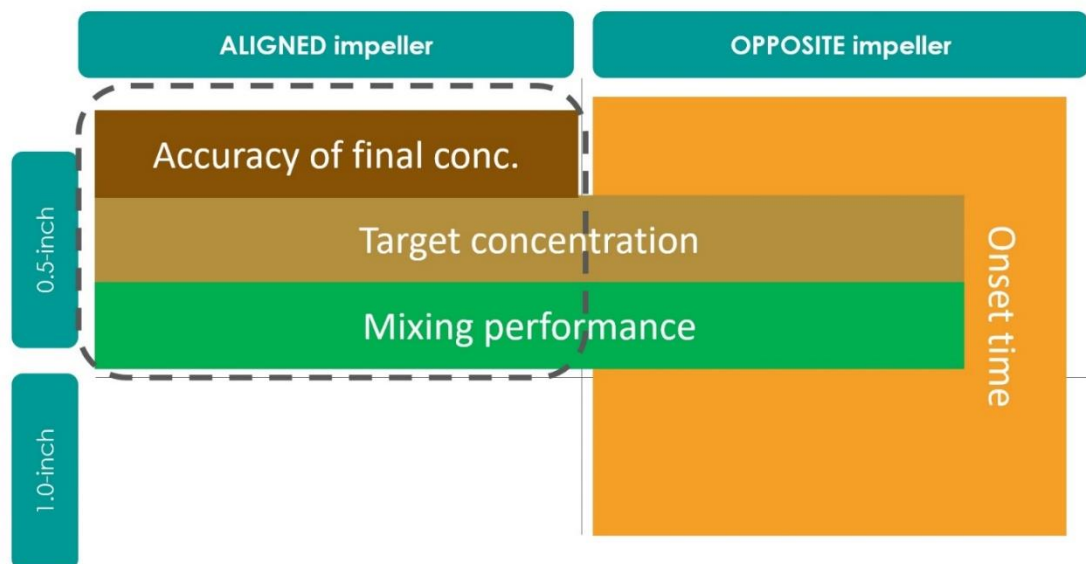


Figure 5-2 Schematic diagram for the best mixing condition.

To increase accuracy of process monitoring with NIRs for future research, the NIR probe should be installed inside the mixer which came directly in contact with the powder to decrease effect of NIRs scattering. Mixing chamber should be made of stainless steel which do not absorb NIRs. Moreover, real-time NIR monitoring should be add to evaluate the finished product from the outlet. Continuous mixer should be developed to include gravimetric and screw feeder to decrease the effect of material flowability and stringent flowrate control.



APPENDIX

Pretreatment of NIR calibration model in the region of 6800 - 8700 cm^{-1}

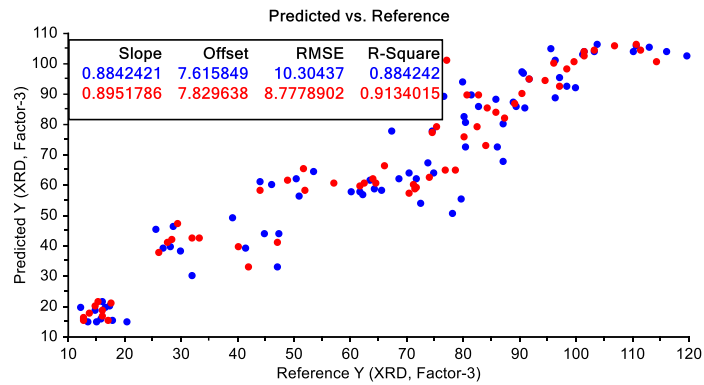


Figure A-1 Calibration model of no. 1 with no pretreatment

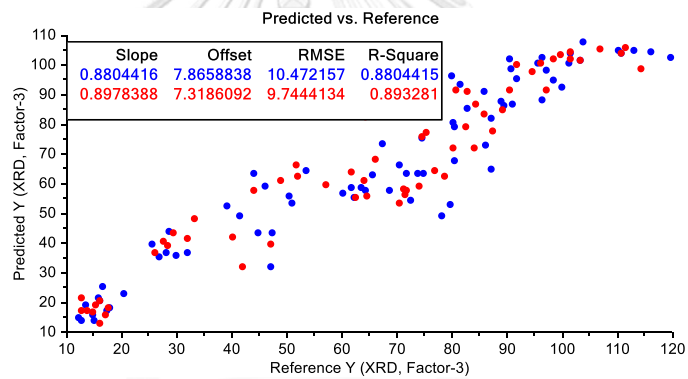


Figure A-2 Calibration model of no.2
with 1st derivative + Norris-Williams pretreatment

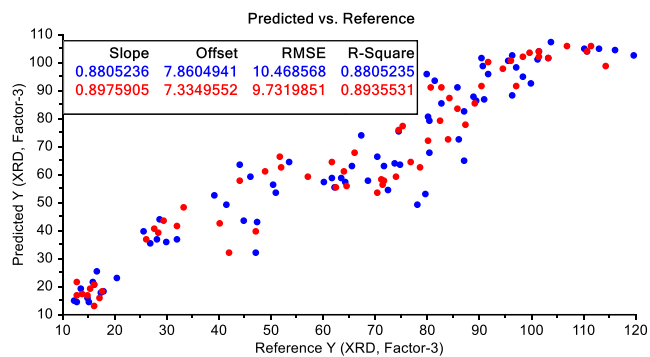


Figure A-3 Calibration model of no.3 with 1st derivative + Savitzky-Golay pretreatment

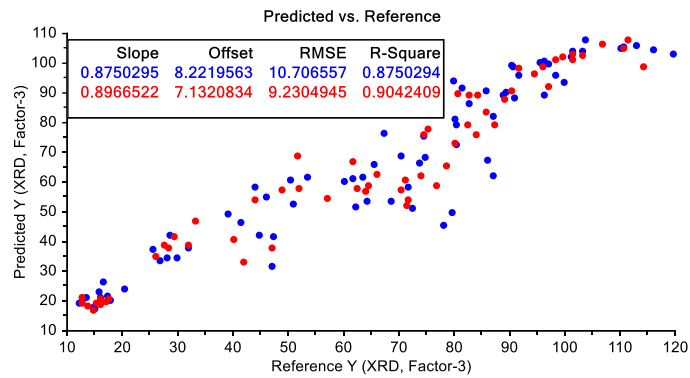


Figure A-4 Calibration model of no.4
with 2nd derivative + Norris-Williams pretreatment

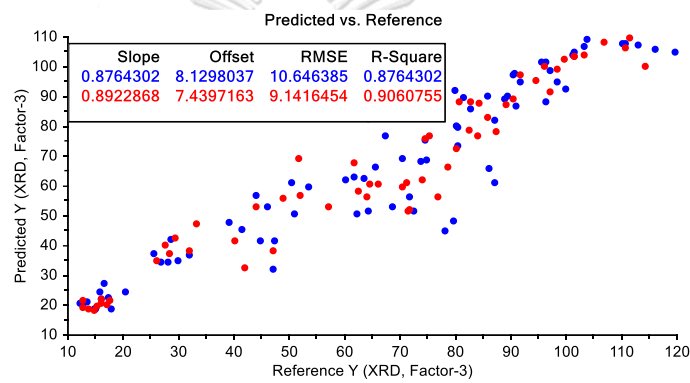


Figure A-5 Calibration model of no.5
with 2nd derivative + Savitzky-Golay pretreatment

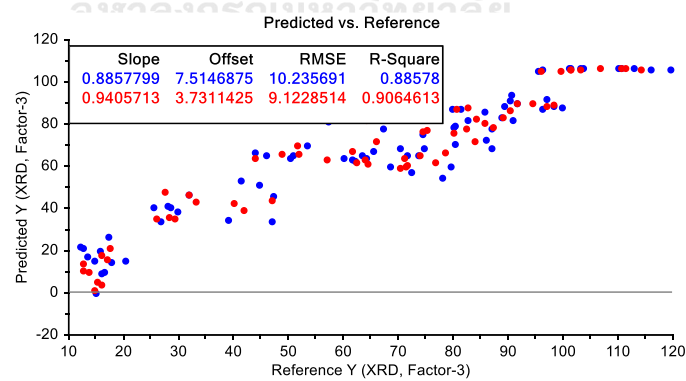


Figure A-6 Calibration model of no.6 with MSC pretreatment

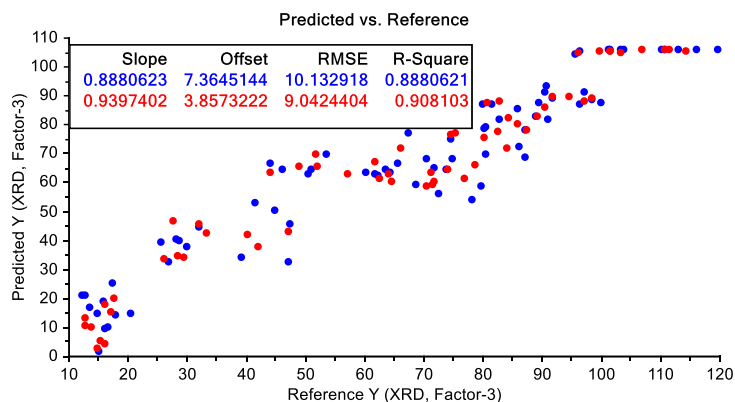
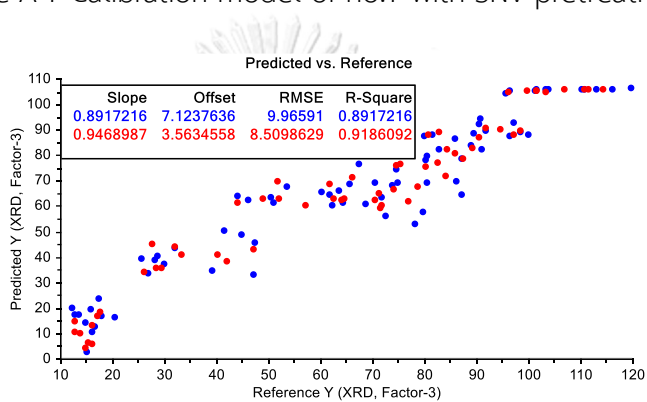
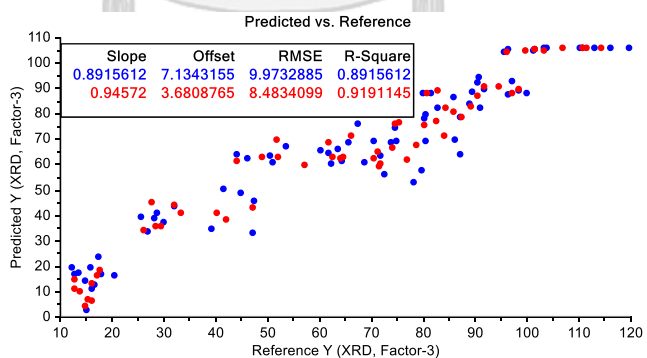


Figure A-7 Calibration model of no.7 with SNV pretreatment

Figure A-8 Calibration model of no.8
with MSC + 1st derivative + Norris-Williams pretreatmentFigure A-9 Calibration model of no.9
with MSC + 1st derivative + Savitzky-Golay pretreatment

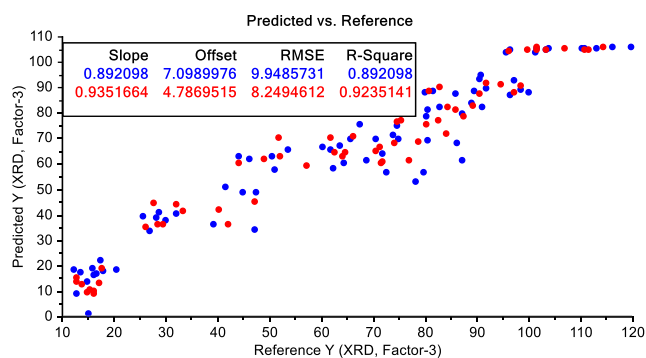


Figure A-10 Calibration model of no.10
with MSC + 2nd derivative + Norris-Williams pretreatment

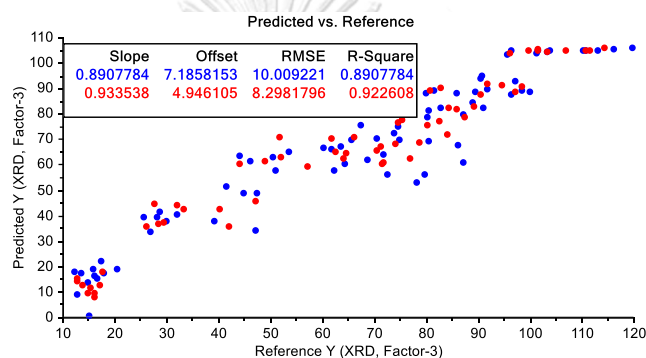


Figure A-11 Calibration model of no.11
with MSC + 2nd derivative + Savitzky-Golay pretreatment

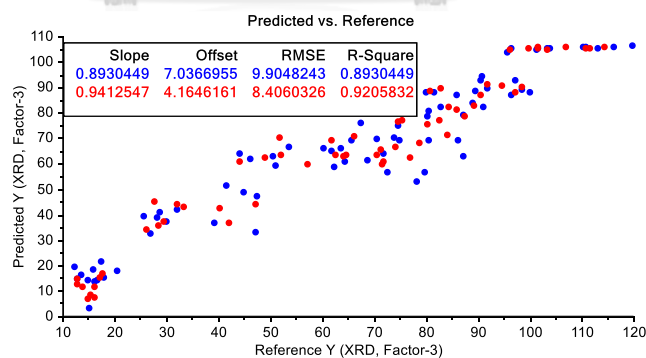


Figure A-12 Calibration model of no.12
with SNV + 1st derivative + Norris-Williams pretreatment

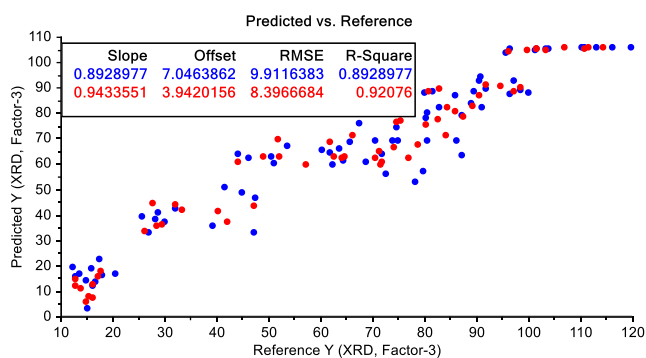


Figure A-13 Calibration model of no.13

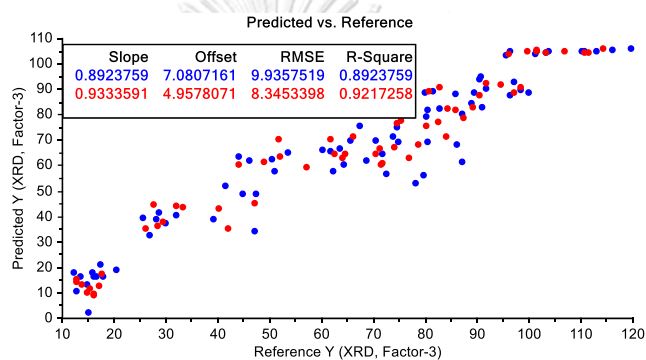
with SNV + 1st derivative + Savitzky-Golay pretreatment

Figure A-14 Calibration model of no.14

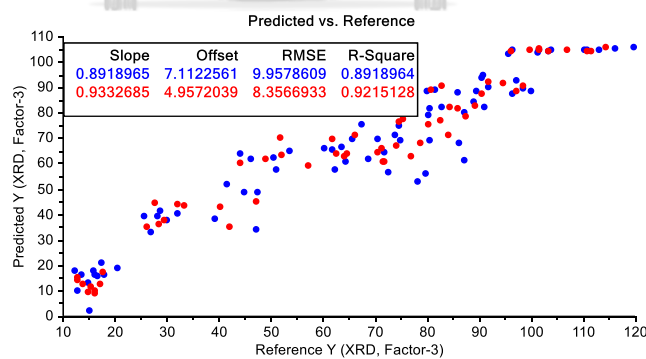
with SNV + 2nd derivative + Norris-Williams pretreatment

Figure A-15 Calibration model of no.15

with SNV + 2nd derivative + Savitzky-Golay pretreatment



จุฬาลงกรณ์มหาวิทยาลัย
CHULALONGKORN UNIVERSITY

REFERENCES

1. U.S. Food and Drug Administration. FDA pharmaceutical quality oversight one quality voice [Available from: <https://www.fda.gov/downloads/AboutFDA/CentersOffices/OfficeofMedicalProductsandTobacco/CDER/UCM442666.pdf>].
2. Plumb K. Continuous Processing in the Pharmaceutical Industry: Changing the Mind Set. *Chemical Engineering Research and Design*. 2005;83(6):730-8.
3. Poux M, Fayolle P, Bertrand J, Bridoux D, Bousquet J. Powder mixing: Some practical rules applied to agitated systems. *Powder Technology*. 1991;68(3):213-34.
4. Manjunath K, Dhodapkar S, Jacob K. Solids mixing, Part B: Mixing of particulate solids in the process industries. In: Paul E.L., Atiemo-Obeng V.A., Kresta S.M., editor. *Handbook of industrial mixing: science and practice*: John Wiley & Sons, Inc.; 2004. p. 924-80.
5. Lee SL, O'Connor TF, Yang X, Cruz CN, Chatterjee S, Madurawe R, et al. Modernizing Pharmaceutical Manufacturing: from Batch to Continuous Production. *Journal of Pharmaceutical Innovation*. 2015;10(3):191-9.
6. Khorasani M, Amigo JM, Bertelsen P, Van Den Berg F, Rantanen J. Detecting blending end-point using mean squares successive difference test and near-infrared spectroscopy. *Journal of pharmaceutical sciences*. 2015;104(8):2541-49.
7. Martínez L, Peinado A, Liesum L, Betz G. Use of near-infrared spectroscopy to quantify drug content on a continuous blending process: Influence of mass flow and rotation speed variations. *European Journal of Pharmaceutics and Biopharmaceutics*. 2013;84(3):606-15.
8. Vanarase AU, Alcalà M, Jerez Rozo JI, Muzzio FJ, Romañach RJ. Real-time monitoring of drug concentration in a continuous powder mixing process using NIR spectroscopy. *Chemical engineering science*. 2010;65(21):5728-33.
9. Vanarase AU, Järvinen M, Paaso J, Muzzio FJ. Development of a methodology to estimate error in the on-line measurements of blend uniformity in a continuous powder mixing process. *Powder technology*. 2013;241:263-71.

10. Järvinen K, Hoehe W, Järvinen M, Poutiainen S, Juuti M, Borchert S. In-line monitoring of the drug content of powder mixtures and tablets by near-infrared spectroscopy during the continuous direct compression tableting process. *European journal of pharmaceutical sciences*. 2013;48(4):680-8.
11. Osorio JG, Vanarase AU, Romañach RJ, Muzzio FJ. Continuous Powder Mixing. In: Cullen PJ, Romañach RJ, Abatzoglou N, Rielly CD, editor. *Pharmaceutical Blending and Mixing*: John Wiley & Sons, Ltd; 2015. p. 100-25.
12. Tannebaum EJ, AIA, Halaby S. Oral solid dosage facilities. In: Jacobs T, Signore AA, editor. *Good design practices for GMP pharmaceutical facilities*. 214. Second ed. Florida: CRC Press; 2017. p. 250.
13. Rooney M. Continuous oral solid dose processing. In: Jacobs T, Signore AA, editor. *Good design practices for GMP pharmaceutical facilities*. 214. Second ed. Florida: CRC Press; 2017. p. 269-94.
14. Myerson AS, Krumme M, Nasr M, Thomas H, Braatz RD. Control Systems Engineering in Continuous Pharmaceutical Manufacturing May 20–21, 2014 Continuous Manufacturing Symposium. *Journal of Pharmaceutical Sciences*. 2015;104(3):832-9.
15. Fonteyne M, Vercruysse J, Leersnyder FD, Van Snick BV, Vervaet C, Remon JP, et al. Process Analytical Technology for continuous manufacturing of solid-dosage forms. *TrAC Trends in Analytical Chemistry*. 2015;67:159-66.
16. Hurter P, Thomas H, Nadig D, Emiabata-Smith D, Paone A. Implementing continuous manufacturing to streamline and accelerate drug development. *AAPS newsmagazine*. 2013:15-9.
17. Tannebaum EJ, AIA, Halaby S. Oral solid dosage facilities. In: Jacobs T, Signore AA, editor. *Good design practices for GMP pharmaceutical facilities*. 214. Florida: CRC Press; 2017. p. 244.
18. Continuous OSD manufacturing - A product & patient perspective [Internet]. ISPE. 2018. Available from: <https://ispe.org/pharmaceutical-engineering/ispeak /continuous-osd-manufacturing-product-patient-perspective>.
19. Muzzio FJ, Alexander A, Goodridge C, Shen E, Shinbrot T. Solids Mixing, Part A: Fundamentals of solids mixing. In: Paul EL, Atiemo-Obeng VA, Kresta SM, editor. *Handbook of Industrial Mixing*: John Wiley & Sons, Inc.; 2004. p. 887-985.

20. Cuq B, Berthiaux H, Gatamel C. Powder mixing in the production of food powders. In: Bhandari B, Bansal N, Zhang M, Schuck P, editor. Handbook of food powders: Woodhead publishing; 2013. p. 200-29.
21. Berthiaux H, Marikh K, Gatamel C. Continuous mixing of powder mixtures with pharmaceutical process constraints. Chemical engineering and processing: process intensification. 2008;47(12):2315-22.
22. Gericke company. Continuous mixing systems with GCM mixers [Available from: https://www.gericke.net/fileadmin/user_upload/_imported/fileadmin/user_upload/PDFs/Prospekte/Englisch/Continuous_Mixing_systems_636_1_UK.pdf].
23. Hosokawa Micron B.V. Brochure: hosokawa mixing technologies [Available from: <https://www.vekamaf.cz/documents/54/Hosokawa%20Micron%20mixing%20technology%20brochure.pdf>].
24. U.S. Food and Drug Administration. Guidance for industry: PAT — A framework for innovative pharmaceutical development, manufacturing, and quality assurance 2004 [Available from: <https://www.fda.gov/downloads/drugs/guidances/ucm070305.pdf>].
25. U.S. Food and Drug Administration. Final Report on Pharmaceutical CGMPs for the 21st Century – A Risk-Based Approach. 2004 [Available from: <https://www.fda.gov/downloads/drugs/developmentapprovalprocess/manufacturing/questionsandanswersoncurrentgoodmanufacturingpracticescgmppfordrugs/ucm176374.pdf>].
26. De Beer T, Burggraeve A, Fonteyne M, Saerens L, Remon JP, Vervaet C. Near infrared and Raman spectroscopy for the in-process monitoring of pharmaceutical production processes. International journal of pharmaceutics. 2011;417(1):32-47.
27. Reich G. Near-infrared spectroscopy and imaging: Basic principles and pharmaceutical applications. Advanced drug delivery reviews. 2005;57(8):1109-143.
28. Ozaki Y, Morita S, Du Y. Spectral Analysis. In: Ozaki Y, McClure WF, Christy AA, editor. Near-Infrared Spectroscopy in Food Science and Technology 2007. p. 47-72.
29. Rinnan Å, Berg FVD, Engelsen SB. Review of the most common pre-processing techniques for near-infrared spectra. TrAC trends in analytical chemistry. 2009;28(10):1201-22.

30. Rajalahti T, Kvalheim OM. Multivariate data analysis in pharmaceuticals: A tutorial review. *International journal of pharmaceuticals*. 2011;417(1):280-90.
31. Roggo Y, Chalou P, Maurer L, Lema-Martinez C, Edmond A, Jent N. A review of near infrared spectroscopy and chemometrics in pharmaceutical technologies. *Journal of pharmaceutical and biomedical analysis*. 2007;44(3):683-700.
32. Porep JU, Kammerer DR, Carle R. On-line application of near infrared (NIR) spectroscopy in food production. *Trends in food science & technology*. 2015;46(2, Part A):211-30.
33. Vanarase AU, Muzzio FJ. Effect of operating conditions and design parameters in a continuous powder mixer. *Powder technology*. 2011;208(1):26-36.
34. Portillo PM, Ierapetritou MG, Muzzio FJ. Effects of rotation rate, mixing angle, and cohesion in two continuous powder mixers—A statistical approach. *Powder technology*. 2009;194(3):217-27.
35. Osorio JG, Muzzio FJ. Effects of processing parameters and blade patterns on continuous pharmaceutical powder mixing. *Chemical engineering and processing: process intensification*. 2016;109:59-67.
36. Meggle. Technical brochure FlowLac® [Available from: <https://www.meggle-pharma.com/en/documents/upload/87/meggle-brochure-flowlac-20140327-en-office.pdf>].
37. Colorcon. Technical bulletin Starch 1500® [Available from: <https://www.colorcon.com/products-formulation/all-products/download/59/116/34?method=view>].
38. Ceolus™. Microcrystalline cellulose: characteristics and function [Available from: https://www.ceolus.com/en/ceolus_ph.html].
39. U.S. Food and Drug Administration. Quality by design for ANDAs: an example for immediate-release dosage forms 2012 [60]. Available from: <https://www.fda.gov/downloads/Drugs/.../UCM304305.pdf>.



จุฬาลงกรณ์มหาวิทยาลัย
CHULALONGKORN UNIVERSITY

VITA

NAME Katesaraporn Wongves

DATE OF BIRTH 9 November 1989

PLACE OF BIRTH Bangkok, Thailand

INSTITUTIONS ATTENDED Bachelor's Degree: Doctor of Pharmacy (Pharm. D),
Huachiew Chalermprakiet University.
Currently studying in Master of Science in Pharmacy
Program in Industrial Pharmacy (M.Sc. in Pharm.), Faculty
of Pharmaceutical Science, Chulalongkorn University.

HOME ADDRESS 120/93 Moo.6 Teparak rd., A.muang, Samutprakarn 10270

PUBLICATION Proceeding in the topic of "Near Infrared calibration model
development for monitoring continuous powder mixing
process." in The 8th National and International Graduate
Study Conference (NGSC&IGSC 2018) " Thailand 4.0
Creative Innovation for Sustainable Development "